SAPIENZA
UNIVERSITÀ DI ROMA

Faculty of Pharmacy and Medicine
Department of Molecular Medicine

PhD in Molecular Medicine

XXXI Cycle

A role for microRNAs/Notch2R network in pediatric High-Grade Gliomas (pHGGs)

Tutor: Prof. Alessandra Vacca

Candidate: Dr. Claudia Sabato

Matr. 1704541

Academic Year 2017-2018

TABLE OF CONTENTS

Abstract

Gliomas represent a very heterogeneous group of tumors that affect the cellular components of the glial system. Pediatric High Grade Gliomas (pHGGs) are a rare, diffusively infiltrating and malignant neoplasms with only few patients achieving long-term survival. Notch signaling is an evolutionarily conserved pathway that regulates many cellular and developmental processes. Its dysregulation has been reported in many pathological contexts, including brain tumours, but little is known about the relevance of Notch signaling in pHGGs. The study of epigenetic mechanism engaged in its regulation could allow a better understanding of mechanisms at the basis of its deregulation.

MicroRNAs are small molecules of 21-24 nucleotides in length and are emerging as major regulators of cancer-related gene expression. Dysregulated microRNAs expression has been implicated in the cancer-related overexpression of several oncogenes.

The present project intends to investigate the functional role of the Notch signaling unveiling epigenetic networks between dysregulated microRNAs and the Notch pathway. Studies on patients'derived pHGG tissues and pHGG cell line, KNS42, revealed down-regulation of three miRNAs, specifically miR-107, miR-181c and miR-29a-3p. This down-regulation increases the proliferation of KNS42 cells by de-repressing expression of the Notch2 receptor, a validated target of miR-107 and miR-181c and a putative target of miR-29a-3p. Inhibition (either pharmacologic or genetic) of Notch2 or re-expression of the implicated microRNAs (all three combined but also individually) significantly reduced KNS42 cell proliferation.

The study reported suggests that Notch2 pathway activation plays a critical role in pHGGs growth and reveals a direct epigenetic mechanism that controls Notch2 expression. These findings identify new molecular targets for more effective treatment of these devastating pediatric brain tumors.

Chapter 1

1.1 Pediatric High-Grade Gliomas

The most common solid tumors of childhood are Central Nervous System (CNS) tumors that account for the majority of cancer related mortality and morbidity.
Among pediatric brain tumors, gliomas are the most frequent with about 30% of incidence (Baker, Ellison, and Gutmann 2016; Ostrom et al. 2017).
Gliomas arise from glial or precursor cells and show an extremely broad range of clinical behavior. The most frequent gliomas are benign and slow-growing lesions, classified as low-grade gliomas (LGG), grade I and II according to criteria established in the World Health Organization (WHO) classification. They are generally curable and show excellent overall survival with current treatments. However, a significant fraction of gliomas develops over a very short period of time and progresses rapidly, they are defined as high grade gliomas (HGGs), grade III and IV by WHO classification.
Pediatric high-grade glioma (pHGG) accounts for 8-12% of all pediatric CNS tumors with an incidence in children up to 19 years of age of about 0.85 per 100000 and a median overall survival of 9-15 months (Jones and Baker 2014; Mackay et al. 2017; Ostrom et al. 2015).
pHGGs may manifest across all ages and anatomic CNS compartments, but most often they arise in midline structures of the brain, where the pons and thalamus are more commonly affected than cerebellum or spine, for which the lack of available surgical options confers an especially poor prognosis. Less frequently they arise in the cerebral hemispheres (Mackay et al. 2017; Sturm, Pfister, and Jones 2017).
The majority of pHGG presents as sporadic tumors with unknown etiology, while others arise in patients with cancer predisposition syndromes, such as constitutional

mismatch repair deficiency (MMR), Li-Fraumeni's syndrome, Neurofibromatosis type 1 (NF1) and Turcot syndrome (Braunstein et al. 2017; Johansson, Andersson, and Melin 2016; Juratli et al. 2018; Sturm et al. 2017).

Pediatric HGG is a rare, malignant, diffusely infiltrating glial neoplasm with very aggressive clinical behavior and comprises a broad spectrum of morphologic aspects (Gajjar et al. 2015). Based on WHO classification, pHGGs essentially encompass anaplastic astrocytoma (AA, WHO grade III) and glioblastoma (GBM, WHO grade IV): the first one is characterized by increased cell density, nuclear atypia and mitotic activity; while GBM also shows microvascular proliferation and necrosis (Braunstein et al. 2017).

1.2 Genetics and epigenetics features of pHGGs

Historically, pediatric HGGs were grouped together with their adult counterpart due to their histological similarities. The latest advances in genomic and epigenome-wide molecular profiling techniques have provided novel insights into the unique genetic and epigenetic alterations of these pediatric neoplasms. Therefore, these achievements have led to a fundamental reclassification of these diseases, moving from an entirely morphology-based categorization to molecular-based separation into subgroups; this could lead to greater diagnostic accuracy, particularly in terms of age at presentation, anatomic location, prognosis and treatment response (Jones et al. 2017).

High-grade gliomas were the first cancer type to be studied and comprehensively profiled by the Cancer Genome Atlas Research Network.

Pediatric HGGs show frequent genetic alterations in the same canonical cancer pathways deregulated in almost all adult GBM, such as the receptor tyrosine kinase (RTK)-RAS-PI3K, the tumor suppressor pathways (TP53 and RB) and finally in

chromatin transcription regulation; however, the precise effectors vary between childhood and adult tumors (Wu et al. 2012, 2014).

The most common structural genomic event, encountered in pHGGs across all brain regions, concerns focal amplification and/or mutation of the RTK, the platelet-derived growth factor receptor α (PDGFRA). Conversely, mutations in epidermal growth factor receptor (EGFR) and in the tumor suppressor PTEN are rare in pHGG (Jones and Baker 2014).

Mutations and loss of the tumor suppressor gene *TP53* have also been identified in pHGGs, where low expression of p53 correlates with improved progression free survival (Braunstein et al. 2017).

Homozygous deletions of cyclin-dependent kinase inhibitor 2A (CDKN2A), focal amplifications of cyclin-dependent kinase (CDK4, CDK6), cyclin D1 (CCND1) and MYC/MYCN have also found in pHGGs, such as amplification of MET and insulin-like growth factor I receptor (IGF1R).

Additionally, pHGGs display very few copy number alterations; in detail, they show recurrent gains of chromosome 1q, lower frequency of chromosome 7 and losses of chromosomes 13q and 14q (Diaz and Baker 2014; Llaguno and Parada 2016).

The greatest and latest hallmark that better illustrates the unique biology of these pediatric neoplasms was the identification of hot-spot somatic histone mutations, that do not play a significant role in the adult disease (Schwartzentruber et al. 2012; Wu et al. 2012).

Histones are the major protein components of eukaryotic chromatin, playing both structural and functional roles. Histones H2A, H2B, H3 and H4 combine as an octamer to compose the nucleosome core and they associate with DNA, via the linker histone H1, to assemble the physiological form of compacted chromatin complex.

Histone tails are substrates for several mechanisms of regulation (methylation, acetylation, ubiquitylation and phosphorylation) that have important effects on the processes of DNA replication, repair and transcription.

In addition to the highly conserved canonical core histones (H2A, H2B, H3 and H4), evidences indicate also the presence of histone variants (Weinberg, Allis, and Lu 2017).

In mammals, histone H3 has three distinct isoforms, namely H3.1, H3.2 and H3.3, that share highly conserved amino acid sequences: histone H3.1 differs from H3.2 by a single amino-acid, serine 96 (Ser^{96}), and H3.3 is distinguished by an additional four amino-acid substitutions serine 31, alanine 87, isoleucine 89 and glycine 90 (Ser^{31}, Ala^{87}, Ile^{89}, Gly^{90}). These histone isoforms play important role in transcriptional regulation and telomere stabilization (Kallappagoudar et al. 2015).

H3.1 and H3.2 represent canonical replication-dependent histones, synthetized and deposited on DNA during the S phase, whereas H3.3 is a non-canonical histone variant. H3.3 is encoded by two isolated genes (*H3F3A, H3F3B*) and it is constitutively expressed in non-dividing cells in a polyadenylated and promoter-dependent manner.

Although the histone variant H3.3 differs from H3.1 and H3.2 in four and five amino-acids residues, respectively, H3.3 is specifically enriched at selected genomic regions, including promoters and gene bodies of highly transcribed genes at specific genomic repeats, such as telomeres and pericentric heterochromatin (Maze, Noh, and Allis 2013).

Moreover, compared with canonical nucleosomes, distinct sets of factors facilitate the assembly and deposition of H3.3 containing nucleosomes.

The histone chaperone Histone Regulator A (HIRA) complex mainly mediates deposition of H3.3 to euchromatic region, whereas its incorporation into pericentromeric and telomeric regions is allowed by H3 chaperones such as α-

thalassemia/mental retardation syndrome X-linked (ATRX) and death-associated protein complex (DAXX).

Specific gain-of-function mutations in the genes encoding H3.3 (*H3F3A*) and H3.1 (*HIST1H3B, HIST1H3C*) histone variants result in amino-acid substitution at two residues in the histone tail: lysine to methionine at position 27 (K27M) and glycine to arginine (G34R) or to valine (G34V) at position 34.

These mutually exclusive histone mutations are associated with distinct anatomical location and patient age.

H3.3 K27M mutation is distributed throughout the CNS midline structures (thalamus, brainstem, cerebellum and spine), while H3.1 K27M is restricted to the pons and H3.3 G34R/V are exclusively found in the cerebral hemispheres (**Figure 1.1**).

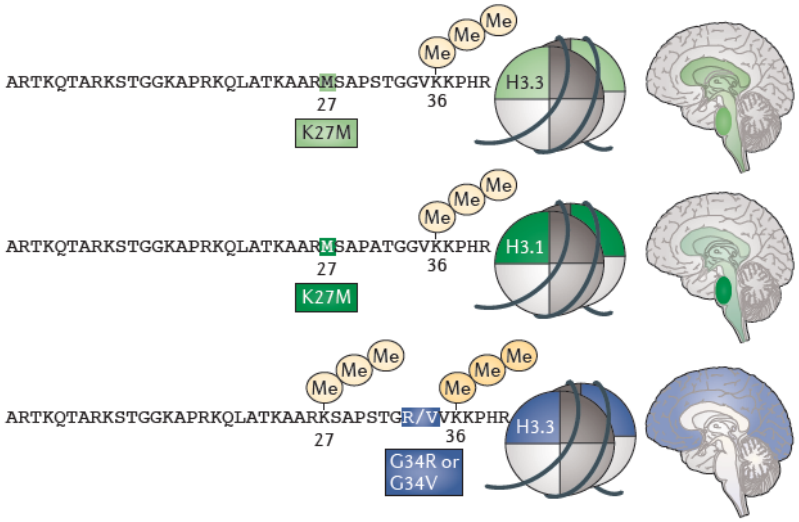

Figure 1.1: Specific recurrent histone mutations in pediatric HGGs and their anatomical location. [from Jones C and Baker S, Unique genetic and epigenetic mechanisms driving pediatric diffuse high-grade glioma. Nat. Rev. Cancer 14, 651–661 (2014)].

The pattern of histone mutations in pHGG also appears to be affected by age: H3.3 K27M mutant tumors are more common in school-age children (median age 11

years), while the H3.1 K27M tends to occur in younger patients (median age 5 years).

On the contrary, H3.3 G34R/V mutations are more prominent in adolescent and young adults (median age 20 years) (Jones and Baker 2014).

Histone mutations differ markedly regarding molecular signature (methylation pattern) and clinical aspects (age of onset, localization and survival).

Among H3.3 mutant tumors, patients with H3.1 K27M mutation have a better prognosis respect those with H3.3 K27M. Whereas comparing the two H3F3A mutations, patients harboring H3G34R/V mutations have a better outcome than patients with K27-mutated GBM. These last data are partially associated to surgical accessibility.

The unique functional consequences that are associated with each of histone mutation result in the disruptions of epigenetic mechanisms; this aspect summarizes the complex interactions between genetic and epigenetic mechanisms of gene transcriptional control. The replacement of lysine with methionine at position 27 decreases methylation at this position and causes a global reduction of H3 di- and tri-methylation, by inhibition of the methyltransferase activity of EZH2, an enzymatic subunit of the polycomb repressive complex 2 (PRC2). For these reasons, transcriptional reprogramming driven by H3 K27M is thought to be the primary oncogenic driver of tumor formation (Lulla, Saratsis, and Hashizume 2016).

In contrast to H3 K27M, H3 G34R/V is not a target of post translational modifications (PTM). It lies in proximity to lysine 36 (K36) so the mutation may interfere with PTM of H3.3 histone tail at position 36 and may promote gliomagenesis, via a more complicated mechanism that involves the decrease of K36me3 and eventually upregulation of NMYC oncogene.

Additionally, each somatic histone mutation is well associated with co-occurring secondary genetic alterations. H3.3 K27M tumors are associated with mutations of FGFR1, largely restricted to thalamus, whereas PDGFRA alterations predominate

in the pons (Fontebasso et al. 2014). These tumors present also differential amplification of CCND2 and CDK4, frequent up-regulation of RTK and *TP53* mutation.

In H3.1 K27M tumors, *TP53* mutations are absent and, notably, there is an enrichment of downstream PI3K pathway mutations, in comparison with the largely upstream RTK alterations present in H3.3 K27M neoplasms. Mutation in ACVR1 - a type I receptor bone morphogenetic protein receptor (BMP) - is often recorded in H3.1 K27 tumor.

Many H3 G34R/V tumors carry concomitant ATRX and/or DAXX and *TP53* mutations. They are the only pediatric subgroup to harbor frequent O^6-Methylguanine-DNA methyltransferase (MGMT) promoter methylation, which encodes a DNA repair enzyme associated with resistance to alkylating agents, such as temozolomide (TMZ).

These achievements allowed to redefine the current concept of molecular pHGG subgroups on the basis of histone mutations. Therefore, the latest updated WHO classification categorizes the newly defined entity termed *diffuse midline glioma H3 K27M-mutant* that includes tumors previously referred to diffuse intrinsic pontine glioma (DIPG) (Jones et al. 2017; Jones and Baker 2014; Juratli et al. 2018; Louis et al. 2016).

Finally, a small subset of hemispheric pHGGs presents gain-of-function mutations in IDH1/2 genes, while another portion carries BRAF V600E mutation.

Mutations of IDH1/2 genes lead to accumulation of the oncometabolite hydroxyglutarate (HG) and disruption of the methylome, due to an extensive DNA hypermethylation at several loci (Chamdine and Gajjar 2014).

Furthermore, in a significant proportion of pHGGs, histone alterations, IDH1/2 or BRAFV600E mutations are absent, thus these entities are classified as H3-/IDH-Wild Type tumors, presenting a remarkably stable genome profile (**Figure 1.2**). These tumors reveal a great molecular intertumoral heterogeneity and can be further

molecularly and prognostically distinct in subtypes with associated oncogenic drivers, as MYCN, PDGFRA and EGFR (Juratli et al. 2018).

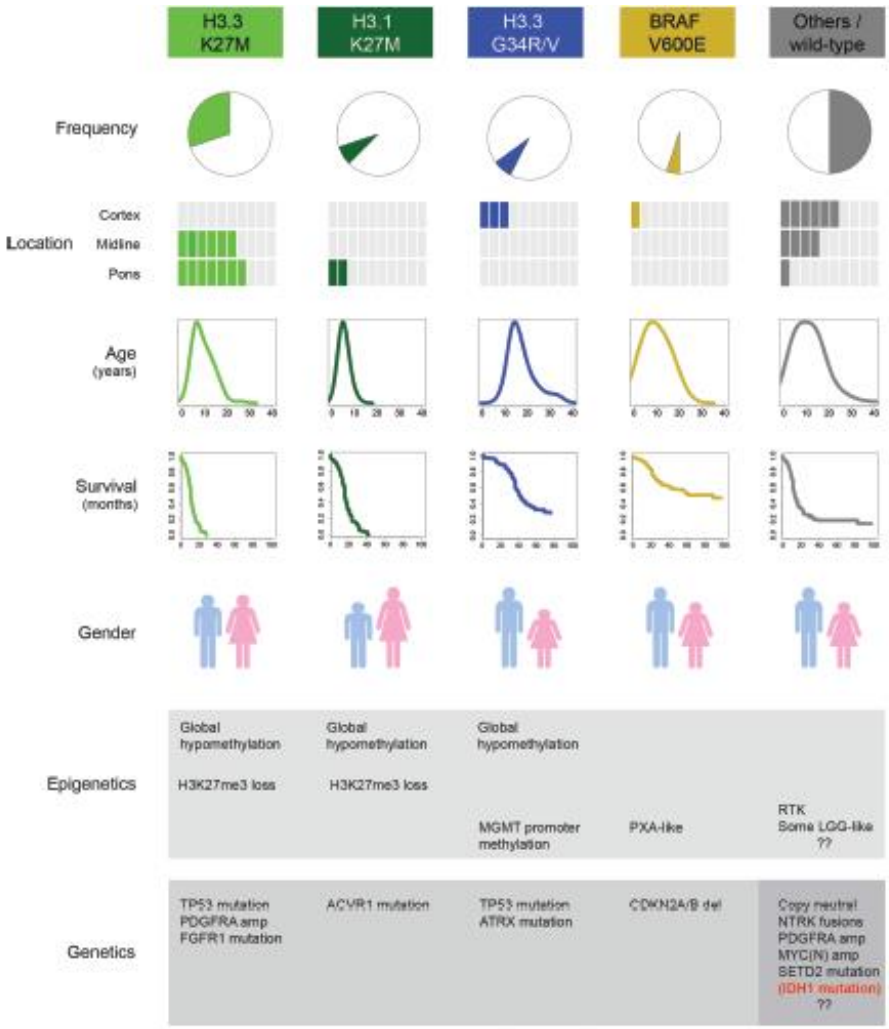

Figure 1.2: **General overview of molecularly defined subgroups in pediatric high-grade gliomas.** For each defined subset, it is indicated the frequency of occurrence, location and age at presentation, clinical outcome, gender distribution, concurrent epigenetic and genetic alterations [from Jones C. et al. Pediatric high-grade glioma: biologically and clinically in need of new thinking, Neuro-Oncology. 19(2), 153-161, 2017].

1.3 Clinical Management

Clinical presentation of a new diagnosis of pHGGs consists of increased intracranial pressure, including persistent headaches, behavior changes, early morning nausea, diplopia and papilledema. In addition, patients may also present localized symptoms, such as focal motor deficits, hemiplegia and dysmetria.

Although molecular and biological knowledge about pediatric HGGs has exponentially increased in a short period of time, its translation into clinical application is lagging.

Several clinical trials have been conducted on pediatric HGGs patients in order to improve treatment outcome of this devastating disease, but unfortunately, little advances have been achieved (El-Ayadi et al. 2017).

Most pHGGs patients still succumb to their disease within 1-3 years after diagnosis, depending on location and molecular signature of the tumor. Standard treatments for GBM and other high-grade gliomas, include maximal safe surgical resection, radio and chemotherapy determining a survival benefit (Chen, Cohen, and Colman 2016).

As a general rule, whenever safe and feasible, gross total resection (GTR) of the tumor by surgery should be attempted. However, a safe complete tumor resection cannot be often achieved, especially for tumors that invade critical structures, namely midline tumors that represent a major proportion of pHGGs cases. Generally, GTR is achievable in only approximately one third of cases.

Several studies have shown that adjuvant radiotherapy and chemotherapy could improve event-free survival (EFS) in children older than three years and in adolescents (El-Ayadi et al. 2017).

A very interesting aspect emerged from the new molecular biology evidences, obtained in pHGGs, is that tumor formation is strongly and frequently associated

with disruption of multiple epigenetic regulatory processes that affect histone modifications, DNA methylation and chromatin remodelers.

These molecular data provide a solid base for the development of novel treatments targeting genetic and epigenetic drivers of pHGG initiation and progression. Unlike genetic mutations, epigenetic alterations are potentially reversible and therefore they have attracted attention for developing drugs against epigenetic enzymes (Gajjar et al. 2015; J.E. and M.J. 2013).

Several agents that target specific chromatin modifiers are in preclinical and/or early clinical development. Several epigenetic drugs have already been approved and tested in hematologic malignancies, where represent a successfully therapeutic option.

More recently, these drugs have increased interest for their use also in gliomas and thus they have been introduced in clinical trials for been accepted also for gliomas treatment.

Chapter 2

2.1 Notch signaling

The Notch signaling is an evolutionarily conserved mechanism that controls an extraordinarily broad spectrum of processes. It plays a pivotal role in the regulation of many fundamental cellular and developmental processes such as proliferation, stem cell maintenance, differentiation during embryonic and adult development and homeostasis of adult self-renewing organs (Artavanis-Tsakonas, Rand, and Lake 1999; Louvi and Artavanis-Tsakonas 2006).

The human Notch family includes four receptors (Notch 1-4) and five ligands (Delta-like-1, Delta-like-3, Delta-like-4, Jagged-1, Jagged-2).

Notch receptors are single pass Type I transmembrane proteins with large extracellular domain (NEC) that contains 29-36 tandem Epidermal-Growth-Factor (EGF)-like repeats, some of which mediate interactions with ligand.

Many EGF repeats bind calcium, which plays an important role in determining the structure and affinity of Notch to its ligand (Cordle et al. 2009; Kopan and Ilagan 2009).

EGF repeats are followed by a unique negative regulatory region (NRR), composed of three cysteine-rich Lin12-Notch repeats (LNR), which plays a critical role in preventing receptor activation in the absence of ligand, and then a heterodimerization domain (HD) (**Figure 2.1**).

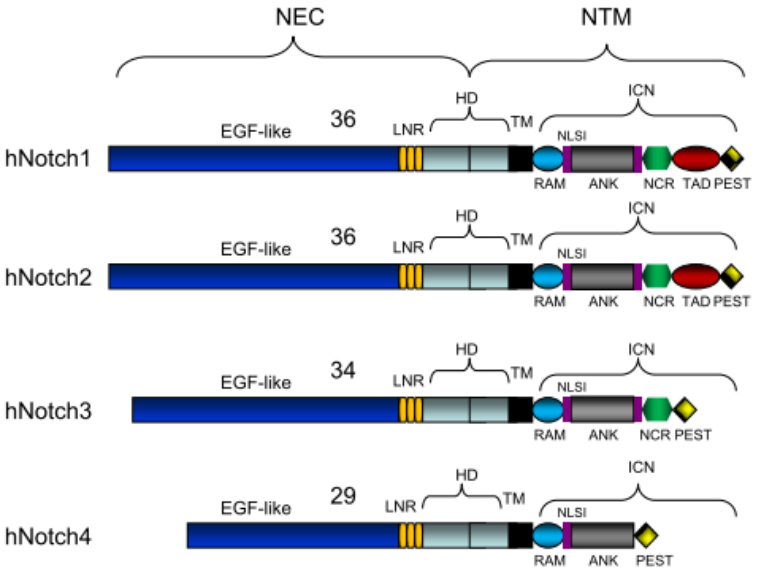

Figure 2.1: Structure of four human Notch receptors.
NEC: extracellular subunit; NTM: transmembrane subunit; EGF: epidermal growth factor; HD: heterodimerization domain; ICN: intracellular domain; LNR: cysteine-rich Lin12-Notch repeats; TM: transmembrane domain; RAM: RBPjκ Association Module domain; NLS: nuclear localizing signals; ANK: ankyrin repeat domain; NCR: cysteine response region; TAD: transactivation domain; PEST: region rich in proline (P), glutamine (E), serine (S) and threonine (T) residues. [From Joanna Pancewicz and Christophe Nicot, BMC Cancer 2011, 11:502].

The Notch extracellular domain is followed by a Notch transmembrane domain (NTM), which is composed by a single transmembrane domain (TM), terminated by a stop translocation signal that includes 3-4 Arg/Lys residues, and intracellularly, by an intracellular domain (ICN).

Notch intracellular domain (NICD) contains a RAM (RBPjκ Association Module) region followed by a linker containing one nuclear localizing sequence (NLS) that links the RAM domain to seven ankyrin repeats (ANK domain). Next to the ANK domain, there are an additional NLS linker and an evolutionarily divergent transactivation domain (TAD).

The very C-terminus contains a highly conserved PEST region (Proline/Glutamic Acid/Serine/Threonine-rich motif) which influences the NICD stability (**Figure 2.1**) (Kopan and Ilagan 2010; Pancewicz and Nicot 2011).

All four Notch receptors are synthesized as single transmembrane polypeptides in the endoplasmic reticulum. Their activity is regulated through post-transcriptional mechanisms (Furin-like protease cleavage at site 1, S1, followed by glycosyl-modifications carried by glycosyltransferase of Fringe family) to produce mature heterodimers then transported to the cell surface through the trans-Golgi network (**Figure 2.2**).

Notch ligands are Type I transmembrane proteins, belonging to the so-called Delta-Serrate-Lag2 (DSL) family. The largest class of Notch ligands is characterized by three related structural motifs: a N-terminal DSL motif, specialized tandem EGF repeats and EGF-like repeats (both calcium binding and non-calcium binding). The DSL domain and the first two EGF-like repeats are necessary for the interaction with EGF-like repeats of Notch receptors and their subsequent activation.

In detail, the activation of the Notch pathway is triggered by ligand binding, presented by neighboring cells, to specific EGF-like repeats (11-12 EGF repeats) of the Notch receptor extracellular domain. The ligand binding induces a conformational change and promotes a sequence of two proteolytic cleavage events in the Notch receptor.

The first one is catalyzed by ADAM-family metalloproteases at site 2 (S2), which is located about 12 amino acids before the TMD and deeply enclosed within the NRR; whereas the second one, at site 3 (S3), is mediated by the γ-secretase–presenilin complex, which cleaves Notch within its NTM and leads to the release of its intracellular domain (referred to as NICD) from the membrane (**Figure 2.2**), (Bray 2006; Kopan and Ilagan 2009, 2010; Teodorczyk and Schmidt 2015).

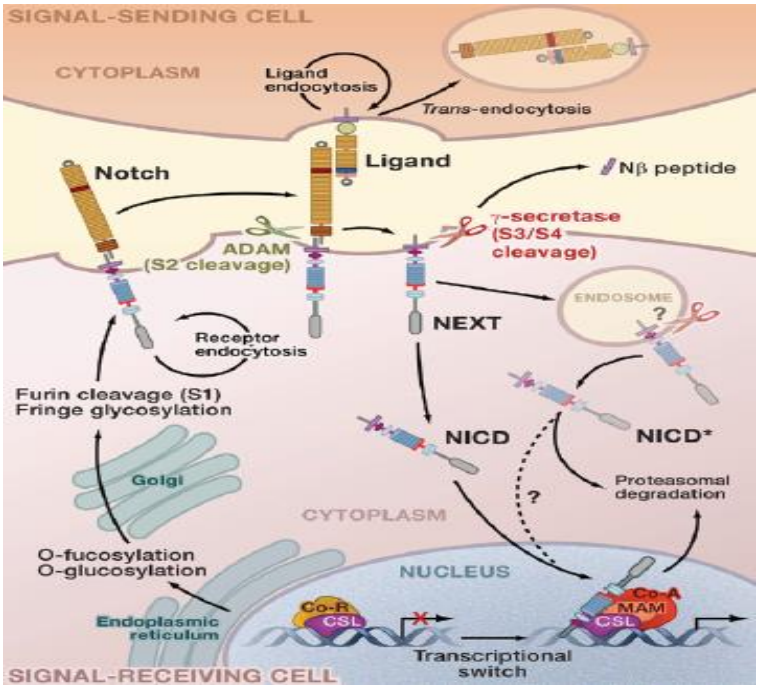

Figure 2.2: Schematic overview of the canonical Notch signaling pathway.
The Notch receptors are produced as large proteins that are cleaved (S1) and inserted in the membrane as heterodimers. Upon ligand binding, two consecutive cleavages occur (S2 and S3), which release the ICN. In the nucleus, ICN forms a multimeric protein complex together with DNA-binding protein (CSL) and co-activators (MAM) and it initiates the transcription of target genes. [From Raphael Kopan and Ma. Xenia G. Ilagan, Cell *137*, 2009].

NICD translocates free into the nucleus where it cooperates with the DNA-binding protein of CSL family (C promoter binding protein-1 in mammals, also referred as RBP-Jk, Suppressor of Hairless of Drosophila, Lag-1 in C.elegans) via its RAM domain.

CSL is a transcriptional regulator that can bind to the consensus DNA sequence, it inhibits transcription gene in the absence of NICD, while it acts as an activator of transcription gene when NICD nuclear translocation happen. The ANK domain, associated with CSL, helps to recruit the coactivator Mastermind-like proteins (MAML 1-3), thereby leading to the transcriptional de-repression of several downstream genes (**Figure 2.2**).

In mammals, the best known Notch target genes are members of the basic helix-loop-helix (bHLH) Hes (Hairy/Enhancer of Split) and Herp (Hes related protein); they are specifically expressed in various tissues and fulfill important roles during development and adulthood. They antagonize early neuronal gene expression, highlighting the central role exerted by Notch in the inhibition of neuronal differentiation (Laug, Glasgow, and Deneen 2018).

Among many others, transcription factors regulated by Notch genes include NFκB, PPAR, c-Myc, Sox2, Pax as well as cell cycle regulators, such as cyclin D1 and p21/Waf1.

Notch pathway is involved in the governance and maintenance of widespread cellular processes.

Aberrant expression of each pathway element, involved in the modulation of the Notch cascade, and gain- or loss- of function mutation of Notch ligand and/or receptor may exert important roles in the development of abnormalities and thus human pathologies.

Dysregulated Notch signaling has been implicated in many tumors both solid, including brain tumors, cervical, lung, pancreatic, breast cancer and hematological malignancies, such as T-cell acute lymphoblastic leukemia (T-ALL), Hodgkin lymphoma and some of the acute myeloid leukemias.

2.2 The role of Notch in gliomas

The formation of the mammalian nervous system takes place via a number of developmental steps that include the recurrent themes of induction, cell proliferation, cell fate determination (differentiation), cell movement (migration), cell process formation and targeting (synapse formation) (Lasky and Wu 2005).

Signaling pathways involved in these processes show a fine space and time regulation; among them the Notch signaling pathway plays a pivotal role in neuro-developmental processes (Bray 2006; Louvi and Artavanis-Tsakonas 2006).

In vertebrates, the primitive neuroepithelium gives rise to two main lineages: neurons and glia. Neurons are generated in embryonic life from multipotent progenitors close to the ventricular zone. After their final mitotic division, neurons migrate away from their birthplace to their ultimate destinations, where they terminally differentiate and become integrated in the brain circuitry. Conversely, glial cells are generated in the proliferating subventricular zone at late embryonic and early postnatal stages (Artavanis-Tsakonas et al. 1999; Bolós, Grego-Bessa, and De La Pompa 2007; Louvi and Artavanis-Tsakonas 2006).

The Notch signaling seems to be involved in neuronal progenitor maintenance (self-renewal) and to govern cell fate differentiation between the neuronal and glial lineages (**Figure 2.3**).

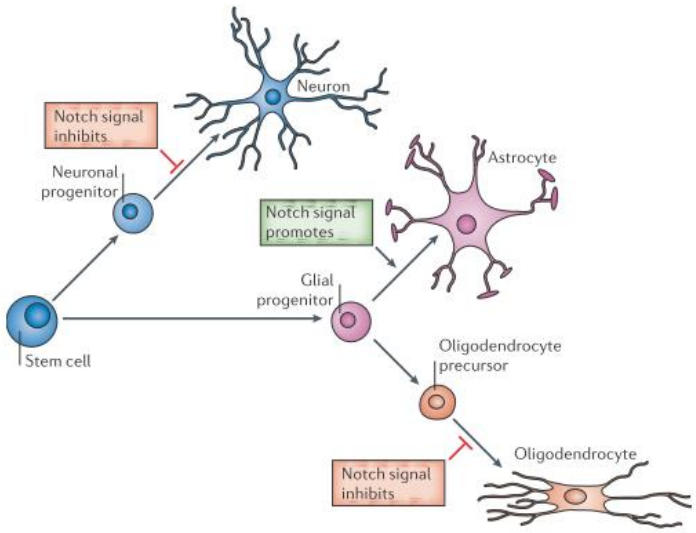

Figure 2.3: Overview of the effect of the Notch signaling activation on cell fate decisions in the vertebrate nervous system.

The self-renewing stem cells can give rise to neuronal progenitors, but their progression to neurons can be inhibited by the Notch signaling activation. Conversely, in gliogenesis Notch seems to have a permissive role, promoting the differentiation into astrocytes, while oligodendrocyte precursors fail to differentiate into mature oligodendrocytes in the presence of active Notch signals. [From Louvi and Spyros Artavanis-Tsakonas, Nature Review, Vol.7, 2006*].*

The Notch signaling inhibits neuronal differentiation, whereas it appears to have a permissive role in gliogenesis, directly promoting the differentiation of many glial subtypes, except for oligodendrocytes. Evidences indicate that deletions of NOTCH effectors and transcription factors (HES1 and HES5) result in premature neuronal differentiation and in a complete loss of glia. Complementary, increases in Notch signaling produce more glia, suggesting its instructive role (Laug et al. 2018).

These implications indicate that gliomas may arise from tumorigenic events within all steps of maturation, from neural stem cell (NSC) to neurons or glia and may display different expression profiles of the Notch signaling cascade components, reflecting the cell of origin (Stockhausen, Kristoffersen, and Poulsen 2010).

Several in vitro and in vivo studies have been conducted in recent years to explore the involvement of the Notch signaling pathway in glioma malignancy (Boulay et al. 2007; Phillips et al. 2006; Purow et al. 2005; Yoon and Gaiano 2005).

Chen *et al.* have reported aberrant activation of Notch signaling in GBM cell lines and human GBM-derived neurospheres, highlighting a differential role for Notch1 and Notch2 receptors with a predominant role of Notch2 (Chen et al. 2010).

Phillips *et al*. have investigated the relation between the Notch pathway and the tumor aggressiveness in a subgroup of high-grade astrocytoma, revealing a prognostic value of Notch pathway markers in pHGGs (Phillips et al. 2006).

These findings indicate that there is a different expression pattern of Notch members among various intracranial neoplasms.

High levels of Notch-1 and its ligands, Delta like-1 and Jagged-1, have been found in many glioma cell lines and primary human gliomas. Immunohistochemical studies of patient-derived tumor tissues indicate that an active Notch signaling is a feature of pHGGs, including those that are negative for Notch1 receptor (Fouladi et al. 2011; Purow et al. 2005).

During the last decades, several classes of Notch inhibitors have been developed to inhibit its activity, mainly composed by γ-secretase inhibitors (GSI), siRNA and

monoclonal antibodies against Notch receptors and its ligands. Furthermore, some Notch-based therapies are in clinical trials.
These inhibitors have used both as a single agent and in combination with targeted or cytotoxic chemotherapy in a subset of patients with brain tumors and they are greatly promising (Capaccione and Pine 2013; Purow et al. 2005; Yuan et al. 2015).

Although the Notch pathway seems to be involved in tumoral initiation and progression of glial neoplasms, the exact genetic and biologic mechanisms through which it results dysregulated are still not better understood. In this scenario, the study of epigenetic mechanisms engaged in its regulation could allow a better understanding of mechanisms at the basis of its deregulation.

Chapter 3

3.1 MICRORNAs

MicroRNAs (miRNAs or miRs) are a key component of the noncoding RNA family, highly conserved across various species of eukaryotes. They are small and single-stranded RNAs, composed of 19-22 nucleotides (Ambros 2004).

MiRNAs exert biological functions by regulating cellular translation and stability of a large number of protein-coding transcripts. The current model suggests that miRISC (miRNA-induced silencing complex) binds to the complementary "seed" region within the 3′ UTR of target RNAs (messenger RNAs) and influences their degradation and/or the level of translation (Bartel 2018).

MiRNA genes are predominantly transcribed by RNA polymerase II as primary miRNAs and processed into precursor and mature forms through a tightly regulated process of biogenesis. Defects in the miRNA biogenesis machinery, such as chromosomal abnormalities, transcriptional control and epigenetic changes lead to their dysregulation (Jansson and Lund 2018).

In the last years, it has emerged that a dysregulated profile of miRNAs expression is associated with alterations of genes involved in the genesis, maintenance and progression of several neoplasms (Di Leva and Croce 2015; Naidu, Magee, and Garofalo 2015).

The identification of specific microRNAs signature in different pediatric brain tumors represents one of the most interesting scientific efforts. In fact, in a previous study Miele *et al*. conducted a high-throughput microRNA profiling of pHGGs showing that a number of dysregulated microRNAs characterized these tumors (**Figure 3.1**), (**Table I**), (Miele et al. 2014).

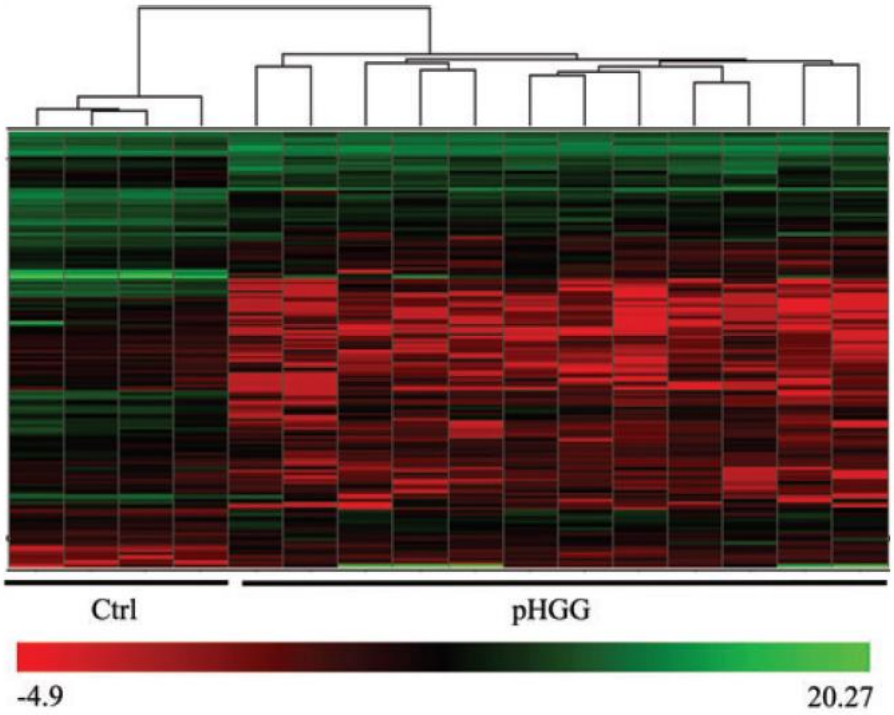

Figure 3.1: Supervised hierarchical clustering of differentially expressed microRNAs between pHGGs and normal brain tissues (CTRL). [From Miele et al. 2014, Nature Review, Neuro-Oncology 16(2), 228–240, 2014].

microRNA	pValue	FDR	FC lin	microRNA	pValue	FDR	FC lin	microRNA	pValue	FDR	FC lin
hsa-let-7a	0,004	0,016	0,334	hsa-miR-193a-3p	0,011	0,029	21,364	hsa-miR-382	0,006	0,019	0,158
hsa-let-7b	0,011	0,029	0,574	hsa-miR-195	0,036	0,071	1,944	hsa-miR-383	0,020	0,046	0,082
hsa-let-7d	0,004	0,016	0,330	hsa-miR-196b	0,015	0,037	0,025	hsa-miR-410	0,036	0,071	0,233
hsa-let-7f	0,004	0,016	0,055	hsa-miR-197	0,004	0,016	0,071	hsa-miR-423-5p	0,011	0,029	0,136
hsa-let-7g	0,048	0,089	0,549	hsa-miR-199a-3p	0,036	0,071	3,839	hsa-miR-425	0,004	0,016	0,026
hsa-miR-100	0,036	0,071	2,137	hsa-miR-19a	0,020	0,061	1,705	hsa-miR-431	0,036	0,071	0,055
hsa-miR-101	0,036	0,071	2,145	hsa-miR-19b	0,021	0,051	1,738	hsa-miR-432	0,018	0,018	0,287
hsa-miR-103	0,008	0,024	0,303	hsa-miR-200a	0,011	0,029	0,041	hsa-miR-433	0,006	0,019	0,065
hsa-miR-106a	0,008	0,024	3,623	hsa-miR-200b	0,011	0,029	0,102	hsa-miR-449a	0,048	0,089	0,135
hsa-miR-106b	0,004	0,016	5,938	hsa-miR-200c	0,027	0,059	0,293	hsa-miR-449b	0,048	0,089	0,093
hsa-miR-107	0,011	0,029	0,094	hsa-miR-202	0,006	0,019	0,013	hsa-miR-450b-5p	0,004	0,016	0,001
hsa-miR-10a	0,008	0,024	0,078	hsa-miR-203	0,008	0,024	0,023	hsa-miR-455-5p	0,020	0,046	5,519
hsa-miR-1183	0,045	0,045	3,843	hsa-miR-204	0,004	0,016	0,101	hsa-miR-484	0,015	0,037	2,292
hsa-miR-1208	0,034	0,034	3,301	hsa-miR-20a	0,036	0,071	1,934	hsa-miR-486-3p	0,004	0,016	0,143
hsa-miR-124	0,020	0,046	0,107	hsa-miR-20a#	0,018	0,018	10,224	hsa-miR-487a	0,004	0,016	0,007
hsa-miR-1253	0,004	0,004	56,190	hsa-miR-21	0,020	0,046	7,522	hsa-miR-487b	0,027	0,059	0,241
hsa-miR-125b-1#	0,006	0,006	30,977	hsa-miR-21#	0,018	0,018	0,049	hsa-miR-489	0,020	0,046	0,177
hsa-miR-126#	0,034	0,034	0,411	hsa-miR-210	0,036	0,071	0,175	hsa-miR-491-5p	0,020	0,046	0,322
hsa-miR-1270	0,018	0,018	0,040	hsa-miR-215	0,004	0,016	0,000	hsa-miR-493	0,011	0,029	0,042
hsa-miR-1275	0,034	0,034	2,637	hsa-miR-218	0,004	0,016	0,095	hsa-miR-494	0,008	0,024	7,996
hsa-miR-128	0,006	0,019	0,104	hsa-miR-219-2-3p	0,004	0,016	0,001	hsa-miR-497	0,045	0,045	2,949
hsa-miR-1282	0,025	0,025	0,032	hsa-miR-219-5p	0,004	0,016	0,002	hsa-miR-501-5p	0,004	0,016	0,004
hsa-miR-129-3p	0,004	0,016	0,004	hsa-miR-22-	0,015	0,037	0,046	hsa-miR-502-5p	0,004	0,016	0,062
hsa-miR-129#	0,004	0,004	0,019	hsa-miR-223	0,036	0,071	3,225	hsa-miR-511	0,048	0,089	0,101
hsa-miR-130a	0,008	0,024	2,194	hsa-miR-23b	0,008	0,024	0,062	hsa-miR-523	0,004	0,016	0,005
hsa-miR-130b#	0,045	0,045	0,107	hsa-miR-24-2#	0,013	0,013	6,866	hsa-miR-532-5p	0,015	0,037	5,438
hsa-miR-132	0,027	0,059	0,214	hsa-miR-25	0,006	0,019	4,327	hsa-miR-539	0,015	0,037	0,177
hsa-miR-133a	0,004	0,016	0,006	hsa-miR-26a	0,006	0,019	0,402	hsa-miR-545	0,008	0,024	0,079
hsa-miR-134	0,020	0,046	0,123	hsa-miR-26b	0,004	0,016	0,297	hsa-miR-576-3p	0,004	0,016	0,053
hsa-miR-136	0,004	0,016	0,008	hsa-miR-27a	0,015	0,037	3,532	hsa-miR-577	0,004	0,004	0,036
hsa-miR-137	0,015	0,037	0,078	hsa-miR-28-3p	0,020	0,046	2,211	hsa-miR-579	0,006	0,019	0,066
hsa-miR-138-2#	0,013	0,013	0,052	hsa-miR-28-5p	0,011	0,029	4,208	hsa-miR-590-3P	0,004	0,004	0,123
hsa-miR-139-3p	0,004	0,016	0,002	hsa-miR-299-5p	0,008	0,024	0,132	hsa-miR-596	0,018	0,018	2,715
hsa-miR-139-5p	0,004	0,016	0,063	hsa-miR-29a#	0,018	0,018	0,075	hsa-miR-625	0,004	0,016	0,103
hsa-miR-140-5p	0,020	0,046	1,996	hsa-miR-301a	0,006	0,019	4,134	hsa-miR-625#	0,004	0,004	0,197
hsa-miR-141	0,006	0,019	0,055	hsa-miR-31	0,015	0,037	0,069	hsa-miR-628-3p	0,025	0,025	0,222
hsa-miR-142-5p	0,020	0,046	0,069	hsa-miR-32	0,004	0,016	0,025	hsa-miR-628-5p	0,027	0,059	0,273
hsa-miR-146b-3p	0,004	0,016	0,003	hsa-miR-320	0,004	0,016	2,070	hsa-miR-636	0,006	0,019	0,037
hsa-miR-148a	0,036	0,071	4,334	hsa-miR-323-3p	0,048	0,089	0,292	hsa-miR-652	0,011	0,029	3,200
hsa-miR-149	0,027	0,059	0,307	hsa-miR-331-3p	0,036	0,071	0,527	hsa-miR-720	0,006	0,006	13,330
hsa-miR-151-5P	0,045	0,045	0,456	hsa-miR-331-5p	0,004	0,016	0,042	hsa-miR-758	0,011	0,029	0,132
hsa-miR-15a	0,048	0,089	5,781	hsa-miR-338-3p	0,004	0,016	0,005	hsa-miR-770-5p	0,013	0,013	0,118
hsa-miR-15b	0,004	0,016	32,381	hsa-miR-340#	0,045	0,045	0,328	hsa-miR-885-5p	0,004	0,016	0,073
hsa-miR-15b#	0,018	0,018	7,654	hsa-miR-342-3p	0,004	0,016	0,230	hsa-miR-888	0,004	0,016	0,001
hsa-miR-17	0,008	0,024	3,146	hsa-miR-342-5p	0,004	0,016	0,012	hsa-miR-92a	0,008	0,024	4,693
hsa-miR-181a-2#	0,034	0,034	2,630	hsa-miR-345	0,011	0,029	3,681	hsa-miR-93	0,008	0,024	3,339
hsa-miR-181c	0,004	0,016	0,104	hsa-miR-346	0,004	0,016	0,002	hsa-miR-95	0,036	0,071	0,210
hsa-miR-187	0,011	0,029	0,022	hsa-miR-34c-5p	0,048	0,089	0,202	hsa-miR-98	0,004	0,016	0,033
hsa-miR-18a	0,011	0,029	7,714	hsa-miR-362-5p	0,015	0,037	0,330	hsa-miR-99a#	0,034	0,034	3,206
hsa-miR-190	0,008	0,024	0,241	hsa-miR-378	0,009	0,009	0,053	hsa-miR-99b	0,004	0,016	0,209
hsa-miR-191	0,036	0,071	0,480	hsa-miR-381	0,048	0,089	0,074				

Table I: List of differentially expressed microRNAs in pHGGs versus normal brain tissues (CTRL). [From Miele et al. 2014, Nature Review, Neuro-Oncology 16(2), 228–240, 2014].

Chapter 4

AIM OF THE STUDY

The present project intends to investigate the functional role of the Notch signaling in pHGGs by using patient derived tissues and a well-characterized in-vitro model of pHGGs that harbors the H3.3 G34V mutation (KNS42 cell line).

Consistent with the growing body of evidence, pointing to microRNAs as major actors in determining dysregulated gene expression in tumors, and as reported in a previous study of Miele *et al.* that indicated several dysregulated microRNAs in pHGGs, the main goal of my project has been to unveil underlying epigenetic networks between dysregulated microRNAs and the Notch pathway.

Chapter 5

MATERIALS AND METHODS

Unless otherwise stated, commercially available products were used according to the manufacturer's instructions / protocols.

5.1 Ethics Statement

The study was conducted in accordance with the Declaration of Helsinki and with the guidelines of the ethical policies of the involved institutions.

5.2 Histology

Formalin-fixed paraffin-embedded (FFPE) samples of 10 pHGGs were obtained from the Pathology Department of the Catholic University of the Sacred Heart and from Sapienza University in Rome. Three-micron-thick sections were stained with hematoxylin and eosin (H&E) for histology. Tumor diagnoses were confirmed by consensus of 3 neuropathologists (F.G., M.A. and M.G.) based on World Health Organization (WHO) criteria (Louis et al. 2016).

5.3 Notch1 and Notch2 immunohistochemistry

Immunohistochemical studies were performed using anti-activated Notch1 (#ab8925, Abcam, Cambridge, UK) and anti-Notch2 antibody (#HPA048743, Atlas Antibodies, Sigma Aldrich, Saint Louis, MO, USA). Paraffin-embedded slices of

adult normal brain tissue purchased from the Biochain Institute (Newark, CA, USA) and of four no autopsy derived healthy brain tissues obtained from the Pathology Department of the Catholic University of the Sacred Heart and from Sapienza University in Rome were used as controls.

The percentage of positive nuclei in each tumor sample and in the glial population of healthy brain tissues was calculated; results were scored as follows: 0 = nuclear positivity rate: 0-10%; 1 = nuclear positivity rate: 11-25%; 2 = nuclear positivity rate: 26-50%; 3 = nuclear positivity rate: 51-75%; 4 = nuclear positivity rate: 76-100% (Munhoz de Paula Alves Coelho et al. 2017).

5.4 Cell lines

Functional studies were performed on KNS42 cells purchased from the Japanese Collection of Research Bioresources Cell Bank. Pediatric low-grade glioma cell lines Res259 and Res186 were kindly provided by Prof. Chris Jones from the Institute of Cancer Research in London. KNS42, Res259 and Res186 cells were grown in DMEM/F12 medium and squamous cell carcinoma (SC-011) were grown in RPMI 1640 medium. All media were supplemented with 10% fetal bovine serum (FBS, Sigma Aldrich, Saint Louis, MI, USA), 2 mM L-glutamine (Gln, Sigma) and 100 units mL^{-1} antibiotic solution (100 units mL^{-1} penicillin and 10000 μg mL^{-1} streptomycin). Cells were cultured at 37 °C in a humidified 5% CO_2 atmosphere.

5.5 Cell Treatments

5.5.1 Pharmacological inhibition of Notch2

KNS42 cells were incubated with GSI (Calbiochem, Merck KGaA, Darmstadt, Germany) at concentrations of 2.5, 5.0 and 10.0 μM and CTRL (0.1% DMSO), harvested after 96 hours of exposure and assayed.

5.5.2 Silencing of Notch2

For the silencing of Notch2 four individual ON-TARGET PLUS siRNA (LQ-012235-00, Dharmacon) were transfected at 100 nM each, or by using the ON-TARGET PLUS SMART pool (code: L-012235-00, Dharmacon). The ON-TARGET PLUS SMART pool yielded the best knockdown efficiency; therefore, it was used for experiments, at the concentration of 100 nM. Silencing of negative control was performed using Silencer Select Negative Control (code: 4390847, Ambion).

All siRNAs were transfected using HiPerfect (Qiagen Inc.). Proliferation was assayed 96 hours after transfection.

5.5.3 MicroRNA overexpression

For single-microRNA overexpression, cells were transfected with 20 nM of one of the following synthetic microRNAs: miR-107 (miRIDIAN microRNA code: C-300527-03, Dharmacon), miR-181c (miRIDIAN microRNA code: C-300556-03, Dharmacon), miR-29a-3p (mirVana miRNA mimic code: MC12499, Ambion-Life Technology, Thermo Scientific, Wilmington, MA, USA); or with negative control (miRIDIAN microRNA negative control code: CN-001000-01-05, Dharmacon). For triple microRNA overexpression treatments, miR-107, miR-181c and miR-29a-3p were used at equal concentrations to obtain a final concentration of 20 nM. All transfections were performed with HiPerfect transfection reagent (Qiagen Inc.). Cells were assayed 48 hours after transfection.

To assess the effects of the treatments described above, KNS42 cells were seeded into 6-well plates (2.5×10^5 cells/well), harvested at the indicated post-treatment time points (24, 48, 72, 96 hours) and subjected to the Trypan Blue exclusion assay,

by counting the number of cells that did not take up trypan blue, to evaluate cell growth.

Res259 and Res186 were seeded into 6-well plates (1.8×10^5 cells/well), harvested after 96 hours and subjected to the Trypan Blue exclusion assay.

5.6 RNA Isolation and qRT-PCR

The isolation of total RNA from fresh-frozen pHGG tissue samples and KNS42 cells have been previously described. For microRNA analysis, single assay qPCR for assessment of miR-107 (code: 002112), miR-181c (code: 000443) and miR-29a-3p (code: 000482) were performed using TaqMan Individual microRNA assays (Applied Biosystems), as previously described (Miele et al. 2014). MicroRNA expression levels were normalized to U6 small nuclear RNA (Thermo Scientific).

5.7 Western Blotting

Western blotting assays were performed as previously described (A. Po et al. 2017) using the following primary antibodies: anti-Notch2 (D76A6) XP #5732 (Cell Signaling, Danvers, MA, USA), anti-NICD2 SAB4502022 (Sigma-Aldrich, St. Louis, MO, USA), anti-Notch1 C-20 sc-6014 (Santa Cruz Biotechnology, Dallas, TE), anti-Sp1 (1C6) sc-420X (Santa Cruz Biotechnology), anti-cleaved PARP G7341 (Promega, Madison, WI, USA), anti-PARP #9542 (Cell Signaling), anti-GAPDH ab-8245 (Abcam, Cambridge, UK) and anti-β-Actin (I-19) sc-1616 (Santa Cruz Biotechnology).

Horseradish peroxidase-conjugated secondary antibodies (Santa Cruz Biotechnology) were used to detect immunoreactive bands, and binding was visualized by enhanced chemiluminescence (Perkin Elmer, MA, USA). ImageJ software was used to perform band densitometry. Protein levels are expressed as

relative to the internal control (β-Actin). Nucleus/cytoplasmic fractionation was conducted as previously described.(Agnese Po et al. 2017).

5.8 Immunofluorescence studies

Immunofluorescence studies were conducted according to standard procedures, as described elsewhere. Briefly, KNS42 cells were plated on glass coverslips and fixed with 4% paraformaldehyde (PFA) for 10 min at room temperature (RT). Fixed cultures were permeabilized and blocked for 30 min with 5% donkey serum (DS) and 0.1% Triton X-100 (Sigma-Aldrich) in phosphate buffered saline (PBS, Sigma-Aldrich). Cells were then incubated overnight with anti-Notch2 antibody (#HPA048743, Sigma-Aldrich). Secondary antibody conjugated with Alexa Fluor 594 (Thermo Fisher Scientific) was diluted 1:200 in PBS with 5% DS and incubated with the specimens for 1 hour at RT. Nuclei were counterstained with Hoechst reagent. After washing, slides were mounted using anti-fade reagent (Dako Fluorescence Mounting Medium, Carpinteria, CA, USA). Images were acquired using a FV1200 MPE laser scanning confocal microscope (Olympus) with a UPlanSAPO 20x/0.75 NA objective. Imaris 8.1 software (Bitplane, Zürich, CH) was used for image processing.

5.9 Plasmid construction and luciferase reporter assay

MiR-29a-3p binding site in 3′-UTR gene regions were identified by bioinformatics analysis using microRNA.org (http://www.microrna.org/microrna/home.do) (Betel et al. 2008, 2010). Human Notch2 3′-UTR (Figure 6.10) was amplified by polymerase chain reaction (PCR).

A region of the human Notch2 3′-UTR (Figure 6.10) containing the putative miR-29a-3p binding site was amplified by PCR using the primers: Notch2 3′-UTR

forward (5′-cactcgagagtccacctccagtgtag-3′) and Notch2 3′-UTR reverse (5′-cagcggccgcagtcaatggaatgcttg-3′) and cloned into psiCheck-2-luciferase reporter vector between the XhoI and NotI sites.

250 ng of the empty psiCheck2 vector or the recombinant plasmid containing the human Notch2 3′-UTR were transiently co-transfected into KNS42 cells with 50 nM of miR-107, used as positive control, or miR-29a-3p or negative control microRNA using Lipofectamine™ 2000 (Invitrogen, Thermo Scientific). Twenty-four hours after transfection, cells were harvested and subjected to the Firefly Luciferase Assay 2.0 (Biotium, Fremont, CA, USA). Cells were incubated in 24-well plates for 15 minutes at room temperature with 100 μl of 1X Passive Lysis Buffer. Subsequently, 20 μl of the lysate was tested with 100 μl of Firefly and Renilla solution in a 96-well plate.

Luciferase activity was detected with a luminometer (GLOMAX). Results are expressed as the ratio of Renilla to Firefly luciferase activity. Reported values are means ± S.D. of values from at least three experiments, each performed in triplicate.

5.10 Statistical Analysis

Data reported in this thesis are the means ± SD of at least three independent experiments each performed in triplicate. Unpaired t-test, Paired t-test, one-way ANOVA and two-way ANOVA were performed wherever appropriate using GraphPad Prism Software version 6.0 (CA, USA), p values < 0.05 were considered to be statistically significant.

Chapter 6

RESULTS

6.1 Notch receptors expression in pHGG

Firstly, nuclear expression levels of the Notch1 and Notch2 was assessed in tissue sections from pHGGs. Sections of normal brain tissue were used as reference control (CTRL).

As expected, based on data reported by Fouladi *et al.*, pHGG tissues displayed weak or any nuclear positivity for the activated form of Notch1 (NICD1), which was comparable to that of the control tissue (**Figure 6.1 A, C**). In contrast, nuclear positivity for Notch2 in the tumor tissues was markedly stronger than that seen in the non-neoplastic brain tissue (**Figure 6.1 B, D**). These findings indicate that pHGGs are characterized by increased levels of activated Notch2 (NICD2) and support the hypothesis that Notch2 receptor plays a functional role in these tumors. Therefore, it was looked for the expression of Notch2 in an in-vitro model of pHGG, the KNS42 cell line.

As shown in **Figure 6.2 A**, immunofluorescence analysis showed that these cells, like the patient-derived pHGG tissues examined by IHC, contained high nuclear levels of Notch2. By counting the number of positive cells nuclei, it resulted that about the 90% of KNS42 expressed Notch2 in the cell nuclei. This finding was confirmed by Western blot analysis performed with a specific antibody for NICD2 (**Figure 6.2 B**) and by performing a nuclear/cytoplasm fractionation assay which demonstrates that NICD2 is only expressed in cell nuclei (**Figure 6.3**).

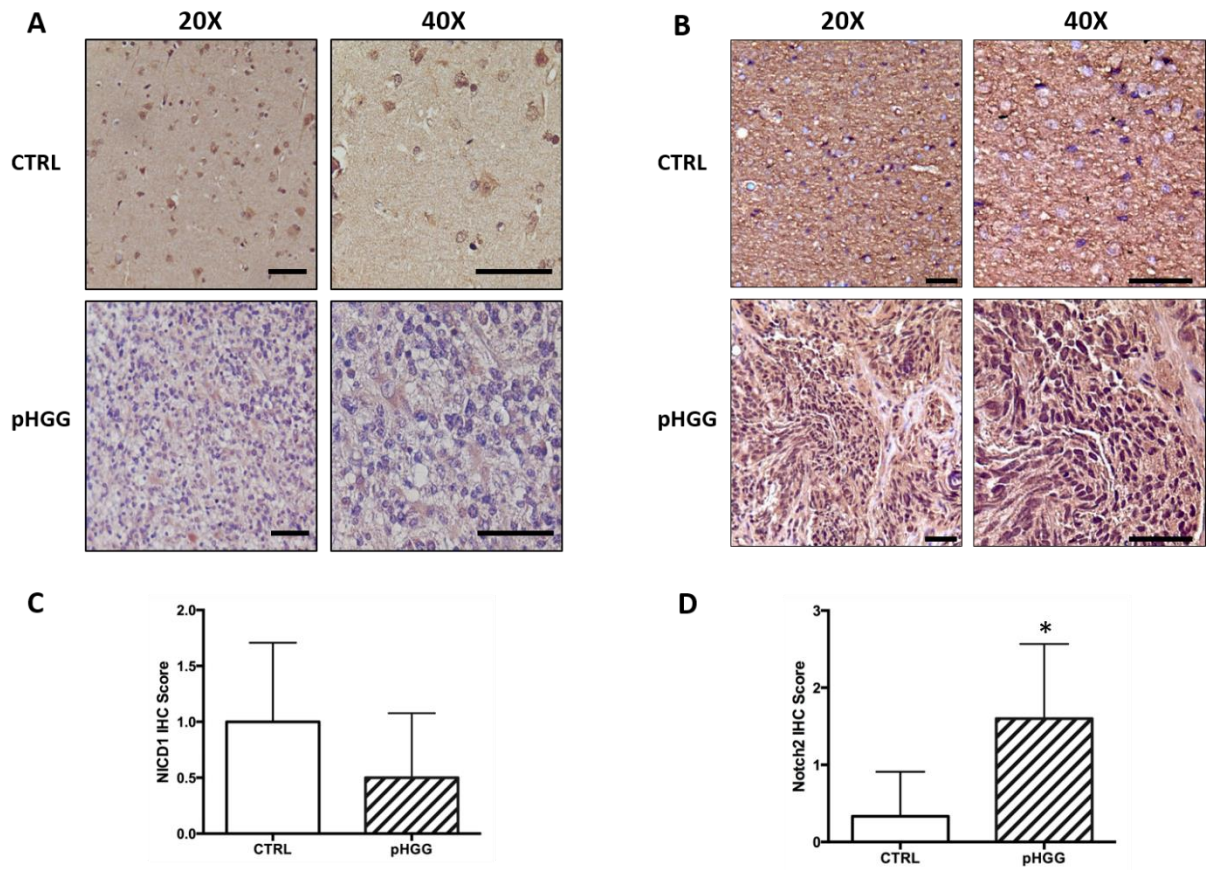

Figure 6.1: Notch1 and Notch2 expression in pHGG and non-neoplastic brain tissues.
Representative images of immunohistochemical (IHC) staining of NICD1 (**A**) and Notch2 **(B)** and relative IHC scores (**C, D**) for nuclear expression of NICD1 and Notch2 in 10 pHGGs and normal brain tissue. * $p<0.05$ vs control (CTRL). Scale bars in (**A, B**): 100 μm.

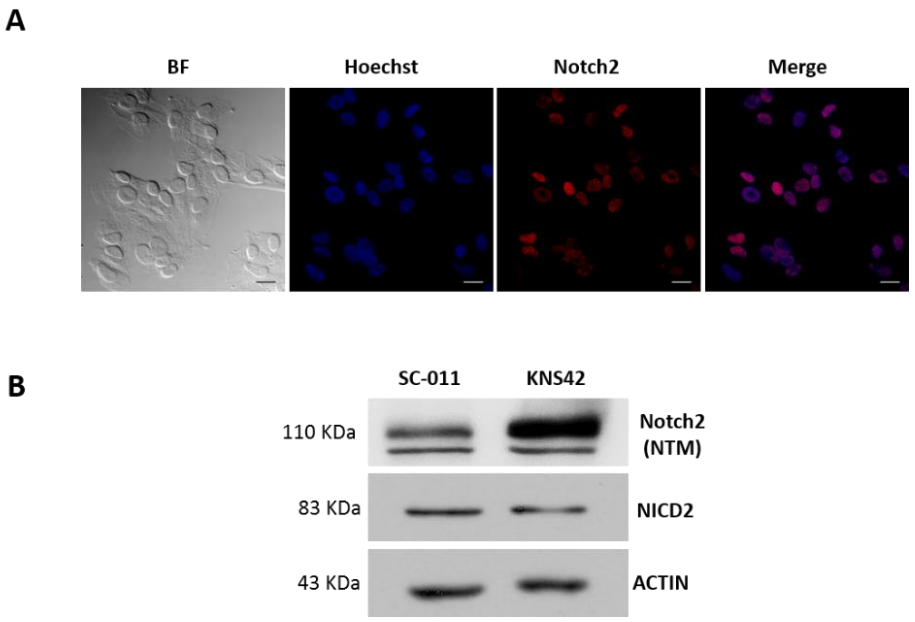

Figure 6.2: Notch2 expression in KNS42 cells line.
(**A**) Immunofluorescence labeling of Notch2 expression in KNS42 cells counterstained with the nuclear marker Hoechst. (BF, bright field.) Scale bars: 20 μm. (**B**) Western blot analysis of the trans-membrane form of Notch2 (Notch2 NTM) and NICD2 levels in KNS42 cells and SC-011 cells (used as positive controls).

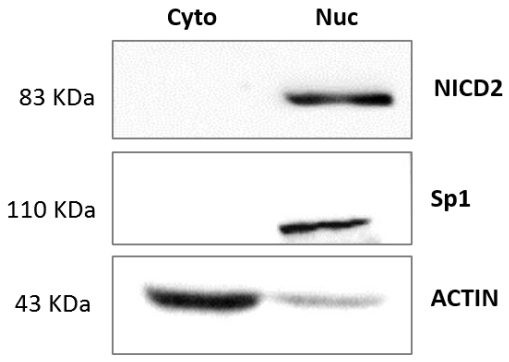

Figure 6.3: NICD2 localization in KNS42 after nucleus/cytoplasm fractionation.
Western blot showing the subcellular localization of NICD2 in KNS42. NICD2 expression was analyzed both in the cytosolic (Cyto) and nuclear (Nuc) fractions. Sp1 and β-actin were used as loading controls and as markers for purity of Cyto and Nuc fractions, respectively.

6.2 Effect of Notch pathway inhibition: the role of Notch2

On the basis of previous results, KNS42 cells were then treated for 96 hours with the gamma-secretase inhibitor (GSI), N-[N-(3,5-difluorophenacetyl)-L-alanyl]-2-phenylglycine *t*-Butyl ester (Mao et al. 2014), which blocks the activity of all four Notch receptors.

Western blot studies revealed dose-dependent reduction of NICD2 levels in treated cells (**Figure 6.4A**). This effect was associated with a decline in cell proliferation, which became significative after treatment with GSI both at 5 and 10 μM (**Figure 6.4 B**). This anti-proliferative effect was due to apoptosis, as demonstrated by the significant increase in the cleaved form of PARP shown in **Figure 6.5**.

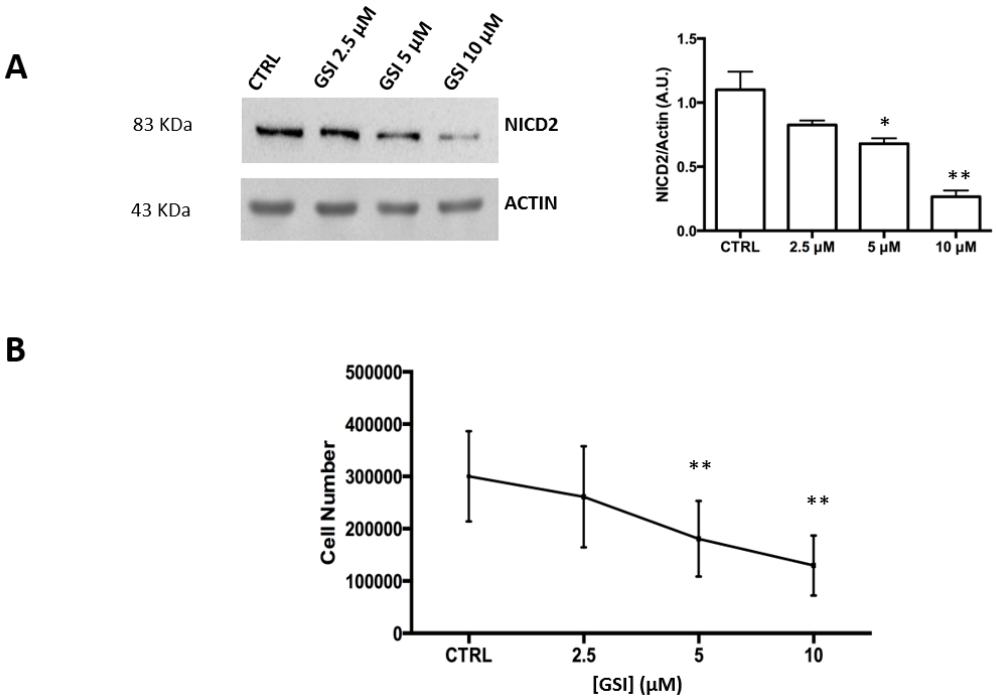

Figure 6.4: Notch2 expression in KNS42 cells line after GSI treatment and the impact of its inhibition on proliferation. (**A-B**) Dose-dependent effects of 96 hours exposure to GSI on (**A**) NICD2 levels and (**B**) proliferation in KNS42 cells line. *p<0.05, **p<0.01 *vs* CTRL (untreated cells in panel A and B).

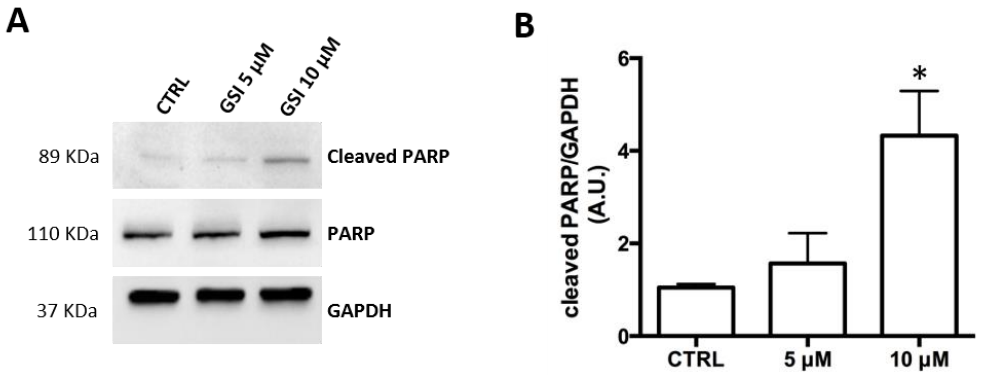

Figure 6.5: Cleaved PARP expression in KNS42 after GSI treatment.
(A) Western blot showing the cleaved and the total form of PARP after 96h of GSI treatment at 5 µM and 10 µM. **(B)** Relative quantification of the level of expression of cleaved PARP after GSI treatment. GAPDH was used as loading control. *p<0.05 *vs* CTRL.

To investigate the contribution of Notch2 inhibition to the effects produced by the GSI, KNS42 cells line was transfected with a siRNA that specifically targeted Notch2 (siNotch2).

It was observed appreciably lower levels of NICD2 in transfected cells (**Figure 6.6 A**) without any reduction of Notch1 expression level, as reported in **Figure 6.6 B**, underlying that siNotch2 was specific to Notch2 only.

The lower levels of NICD2 were associated with significant decreases in cell proliferation, which were already evident 72 hours after siNotch2 silencing (**Figure 6.6 C**).

Collectively, these results confirm the assumption that Notch2 plays a substantial role in the Notch-mediated control of pHGG cell proliferation.

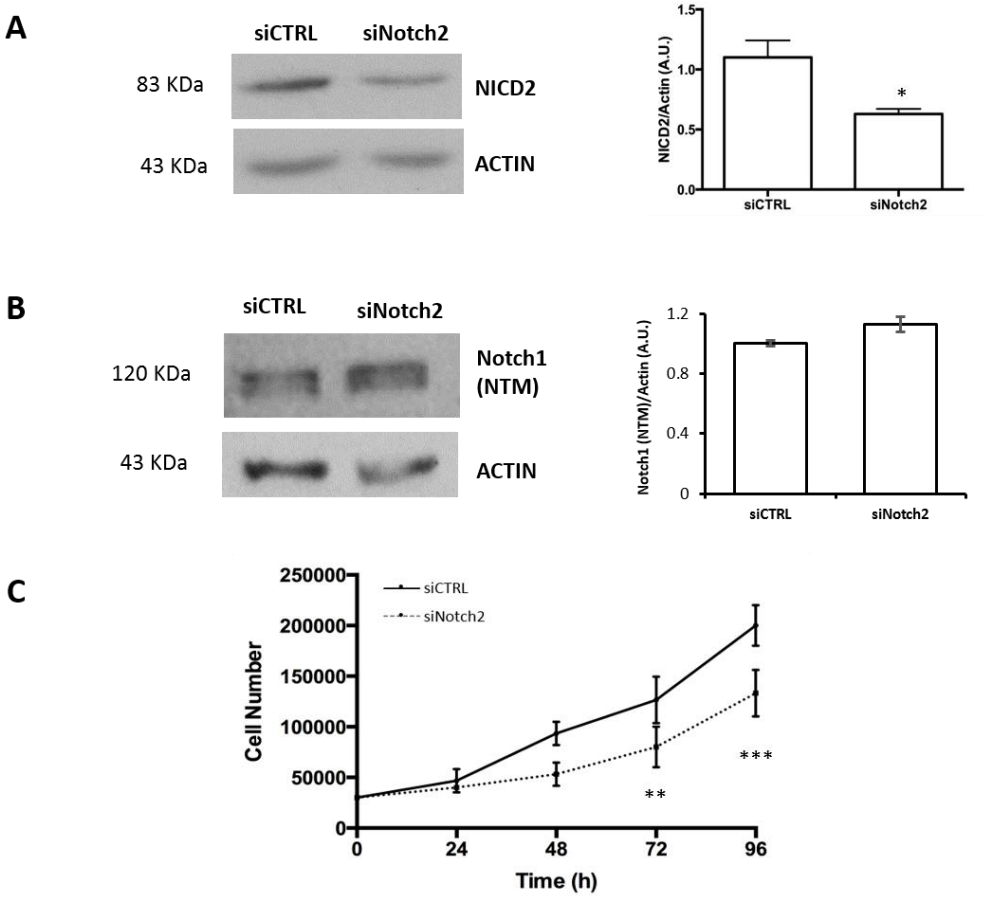

Figure 6.6: Effects of siRNA-mediated knockdown of Notch2 in KNS42 cells line.
(**A**) Western blot analysis of NICD2 levels 96 hours after transfection and relative densitometric analysis. (**B**) Western blot analysis of Notch1 levels 96 hours after Notch2 silencing in KNS42 cells and densitometric analysis. (**C**) Time-course of the effects of Notch2 silencing on KNS42 cell proliferation. *p<0.05, **p<0.01, *** p<0.001 *vs* CTRL (silencing negative control-transfected cells).

6.3 MicroRNAs expression in pHGG cell line

Dysregulated microRNA expression has been implicated in the cancer-related overexpression of numerous oncogenes. A previous study of my group has already shown that multiple microRNAs are differentially expressed in pHGGs (Miele et al. 2014).

To investigate the mechanism underlying the increased levels of Notch2 expression in pHGG cell line, the resulted list of microRNAs that had displayed down-regulated expression in pHGGs versus normal brain tissue was previously examined (Table I indicated above).

Interrogation of miRTarBase and microRNA.org revealed Notch2 to be a validated target of two of the microRNAs on this list (miR-107 and miR-181c) and a putative target of a third, miR-29a-3p [(http://mirtarbase.mbc.nctu.edu.tw) (microRNA.org)]; (Chen et al. 2013; Chou et al. 2016; Hashimoto et al. 2010).

Consistent with previous findings in pHGGs (Miele et al. 2014), all three of these microRNAs were expressed at significantly lower levels in KNS42 cells than in non-neoplastic brain tissues (CTRL) as shown in **Figure 6.7**.

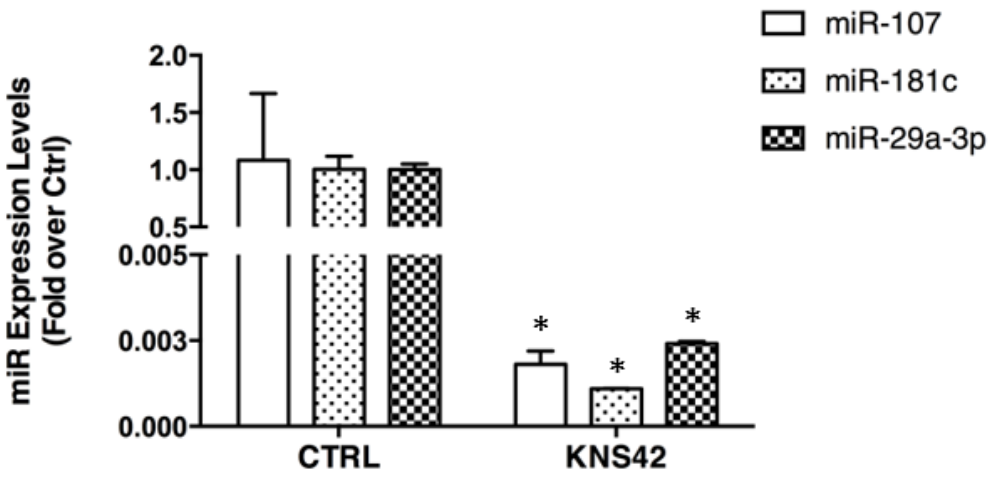

Figure 6.7: MiR-107, miR-181c and miR-29a-3p expression levels in KNS42.
Single assay qPCR validation of miR-107, miR-181c and miR-29a-3p expression in KNS42 cells versus non-neoplastic total brain (CTRL). *p<0.05 *vs* CTRL.

6.4 Effect of miRNA re-expression in pHGG cell line

To analyze the biological impact of microRNAs down-regulation, they were overexpressed, individually and combined, in KNS42 cell line.

After verifying the physiological range of their re-expression levels by RT-qPCR (**Figure 6.8 A**), it was assessed the ability of the microRNAs to diminish NICD2 protein levels.

As shown in **Figure 6.8 B**, both over-expression of each microRNA and their combination significantly decreased protein levels of NICD2. Based on the previous findings, respectively shown in Figure 6.4 and Figure 6.6, it was expected that overexpression of these microRNAs would also be associated with reduced pHGG cell proliferation. Trypan blue exclusion assays showed that KNS42 cell death was not significantly affected by overexpression of any of the microRNAs, even when combined.

In contrast, as shown in **Figure 6.8 C**, by post-transfection hour 72, proliferation was already significantly decreased in cells overexpressing all three microRNAs or miR-181c alone. By 96 hours these reductions were even more evident, the effect was also statistically significant for cells overexpressing miR-107 or miR-29a-3p alone.

Importantly, at both time points, the anti-proliferative effect was more substantial in cells subjected to combined overexpression of the three microRNAs, indicating that miR-29a-3p, miR-107 and miR-181c may act synergically to check KNS42 cell proliferation.

Furthermore, the role of these three microRNAs was analyzed in other two immortalized cell lines derived from different glioma grades.

Specifically, for the scope were used two pediatric low-grade glioma cell lines: Res259, derived from a grade II diffuse astrocytoma, and Res186, derived from a

grade I pilocytic astrocytoma. Firstly, the expression levels of miR-29a-3p, miR-107 and miR-181c were evaluated in Res259 and Res186.

As shown in **Figure 6.9 A**, their expression levels were comparable to that one found in KNS42 cells. Then, as reported in **Figure 6.9 B-C**, the ability of these microRNAs in reducing cell proliferation was assessed after their re-expression in both the pediatric low-grade glioma cell lines.

Respectively, Res259 cells seem to be more sensitive than Res186. Cell proliferation indeed was significantly affected by the overexpression of all microRNAs, except miR-181c in Res259; while in Res186 only miR-29a-3p and the combined overexpression of the three microRNAs induced a significant effect. The anti-proliferative action of these microRNAs in Res259 and Res186 cells did not increase after 96h in respect to what it was observed at 48 hours.

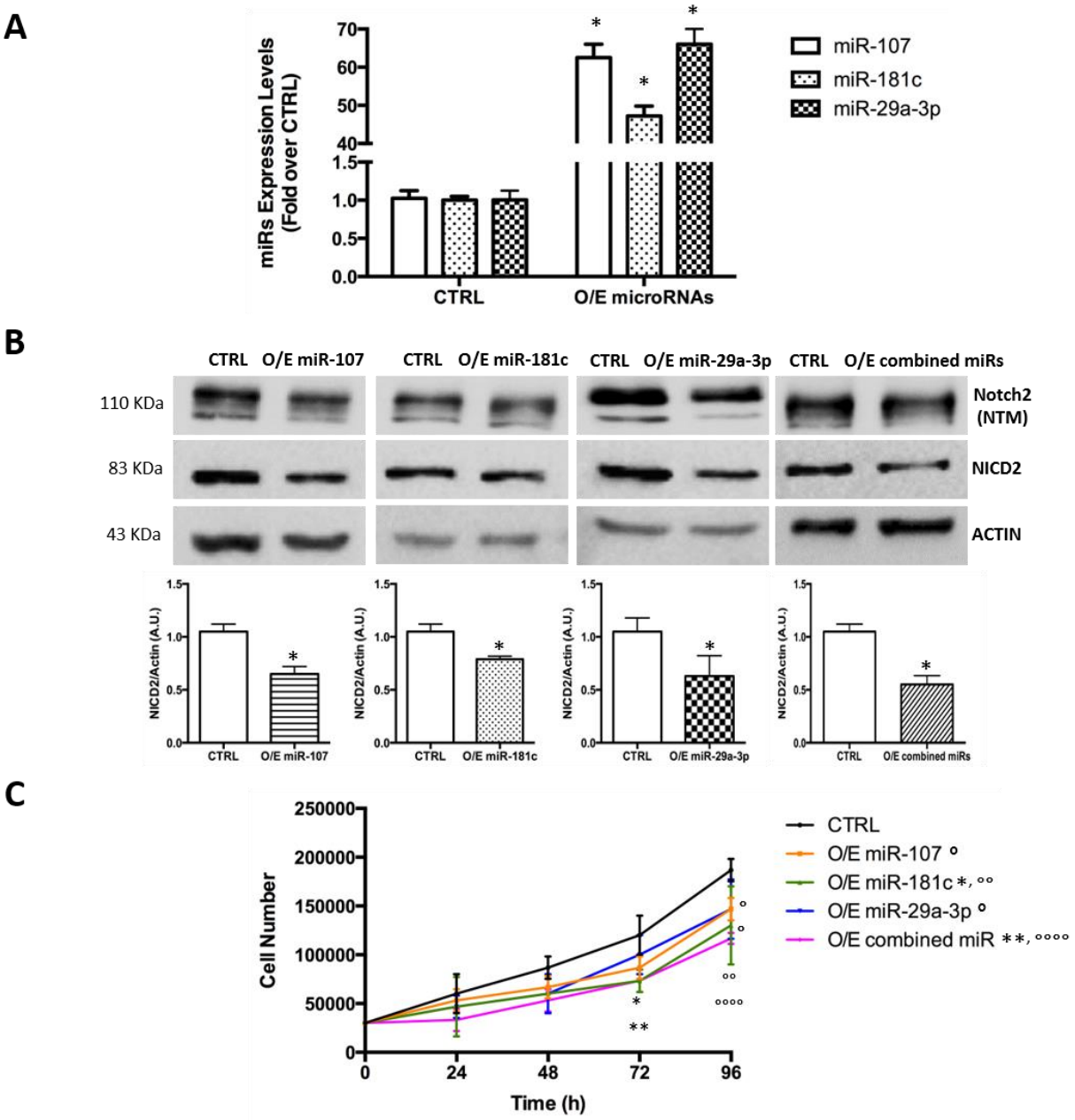

Figure 6.8: MiR-107, miR-181c and miR-29a-3p inhibit pHGG cell proliferation by targeting Notch2.

KNS42 cells were transfected with 20 nM of miR-107, miR-181c and miR-29a-3p: pre-transfection (CTRL) and 48 hours-post-transfection (O/E) levels of (**A**) each microRNA and (**B**) of the trans-membrane form of Notch2 (Notch2 NTM) and NICD2 with relative densitometric analysis. *p<0.05 *vs* CTRL. (**C**) KNS42 cell proliferation after O/E of the three microRNAs, separately and combined. Significant differences vs. CTRL at 72 hours (*p<0.05, **p<0.01) and at 96 h (°p<0.05, °°p<0.01, °°°p<0.001, °°°°p<0.0001).

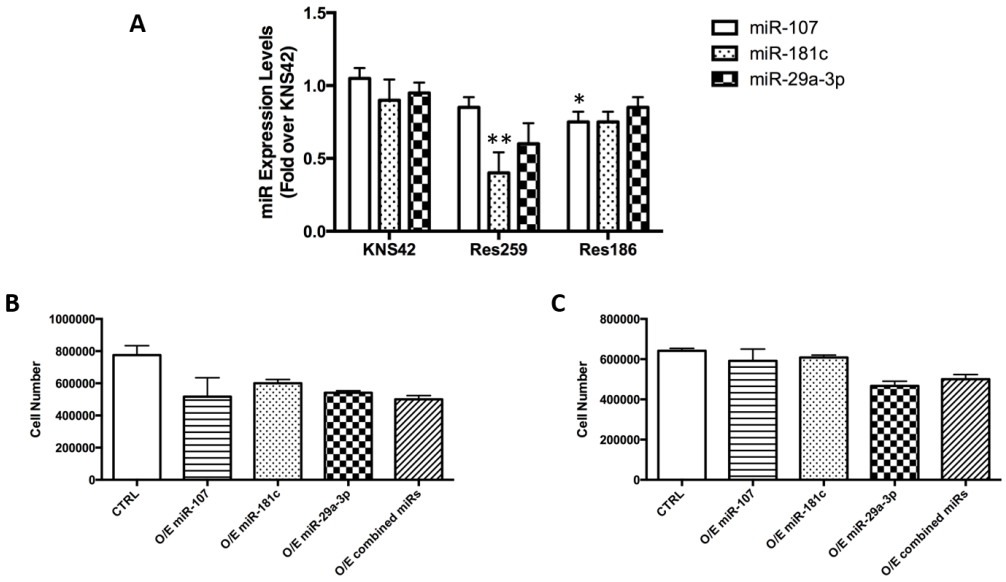

Figure 6.9: MiR-107, miR-181c and miR-29a-3p inhibit glioma cell proliferation.
(**A**) Single assay qPCR of miR-107, miR-181c, and miR-29a-3p expression in KNS42 cells versus Res259 and Res186, a grade II and a grade I pediatric glioma derived cell lines, respectively. (**B-C**) Res259 (**B**) and Res186 (**C**) cells were transfected with the three microRNAs, separately and combined. Cell proliferation was evaluated 48 hours-post-transfection. (**A**) *p<0.05, **p<0.01 *vs* KNS42. (**B-C**) *p<0.05, **p<0.01 *vs* CTRL**.**

6.5 Evaluation of miRNAs target sites by functional luciferase assay

As noted above, unlike miR-107 and miR-181c (Chen et al. 2013; Chou et al. 2016; Hashimoto et al. 2010), the binding of miR-29a-3p to the 3'-UTR of Notch2 has been never experimentally validated. To address this gap, a portion of the Notch2 3'UTR containing the putative binding site for miR-29a-3p was cloned into a luciferase reporter vector and transfected into KNS42 cells (**Figure 6.10**).

gagtccacctccagtgtagagacataactgacttttgtaaatgctgctgaggaacaaatgaaggtcatccgggagagaaatgaagaaa
tctctggagccagcttctagaggtaggaaagagaagatgttcttattcagataatgcaagagaagcaattcgtcagtttcactgggtatc
tgcaaggcttattgattattctaatctaataagacaagtttgtggaaatgcaagatgaatacaagccttgggtccatgtttactctcttcta
tttggagaataagatggatgcttattgaagcccagacattcttgcagcttggactgcattttaagccctgcaggcttctgccatatccatg
agaagattctacactagcgtcctgttgggaattatgccctggaattctgcctgaattgacctacgcatctcctcctccttggacattcttttg
tcttcatt**tggtgct**tttggttttgcacctctccgtgattgtagccctaccagcatgttatagggcaagacctttgtgcttttgatcattctggc
ccatgaaagcaactttggtctcctttcccctcctgtcttcccggtatcccttggagtctcacaaggtttactttggtatggttctcagcacaa
acctttcaagtatgttgtttctttggaaaatggacatactgtattgtgttctcctgcatatatcattcctggagagagaaggggagaagaat
acttttcttcaacaaattttgggggcaggagatcccttcaagaggctgcaccttaatttttcttgtctgtgtgcaggtcttcatataaacttt
accaggaagaagggtgtgagtttgttgtttttctgtgtatgggcctggtcagtgtaaagttttatccttgatagtctagttactatgaccctc
cccacttttttaaaaccagaaaaaggtttggaatgttggaatgaccaagagacaagttaactcgtgcaagagccagttacccacccaca
ggtccccctacttcctgccaagcattccattgactgc

Figure 6.10: Region of the Notch2R 3'UTR cloned in the luciferase reporter vector.
Underlined and bold is the binding site for miR-29a-3p.

As shown in **Figure 6.11**, re-expression of miR-29a-3p in these cells significantly reduced expression of the reporter gene in the recombinant vector containing the 3'-UTR of Notch2.

This finding thereby provides the first experimental evidence that miR-29a-3p is a direct negative regulator of Notch2 expression.

Taken together, these observations confirm that high levels of Notch2 in pHGG cells are sustained, at least in part, by the down-regulated expression of miR-107, miR-181c and miR-29a-3p.

```
5′-..UCUUUUGUCUUCAUUUGGUGCUU..
                ||||   |||||||
3′-...AUUGGCUAAAGUCUACCACGAU..
```

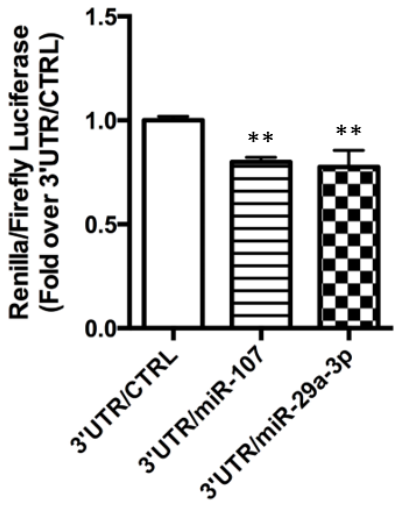

Figure 6.11: Renilla activity induced by ectopic expression of Notch2 and negative control (CTRL) in KNS42 cells transfected with Renilla vector bearing the Notch2 3′UTR.
MiR-107, whose targeting of Notch2 has been previously validated, was used as positive control. Results are expressed as the ratio of Renilla to Firefly luciferase activity. * $p<0.05$ *vs* 3′UTR/CTRL.

Chapter 7

Discussion

MicroRNAs are critical components of the post-transcriptional machinery that regulates tumor cell growth (Dawson and Kouzarides 2012; De Smaele, Ferretti, and Gulino 2010).

In the present thesis was identified a microRNA-based mechanism that activates proliferative Notch2 signaling in pHGGs.

To the best of our knowledge, to date, only two studies have investigated the role of Notch signaling in pHGGs. In 2011, Fouladi *et al.* reported that FFPE sections of grade III and IV malignant gliomas removed from pediatric patients displayed intense nuclear staining for two transcription factors that are downstream effectors of the Notch pathway, HES1 and HES5, and this positivity was also observed in those tumors that were immunonegative for the Notch1 (Fouladi et al. 2011).

More recently, Dantas-Barbosa *et al.* (2015) showed that pediatric glioma xenografts and the pediatric glioma cell line, SF188, express Notch1, the Notch ligand (*DLL1*) and several of Notch pathway's downstream target genes (*HES1, HEY1, MYC and FBXW7*), but neither pharmacological nor genetic blockade of Notch1 was capable of reducing pHGG cell growth. Nevertheless, *MYC* resulted to be over-expressed in these pediatric glioma xenografts. Therefore, even though literature studies are not numerous, both of them reports evidence that Notch pathway is active in pHGGs.

The Notch signaling pathway is a highly conserved pathway that plays major role in many cellular processes; its function is strongly cell context-dependent (Artavanis-Tsakonas et al. 1999). Notch signaling can play oncogenic as well as oncosuppressive role in tumorigenesis; the four Notch receptors are also

characterized by functional diversity, even within the same biological setting (Nowell and Radtke 2017).

The present study is the first attempt to delineate the specific role of Notch2 in pHGGs. The increased nuclear levels of NICD2 - the active form of the protein - shown in pHGGs (patient-derived tissues as well as the KNS42 cell line), support a role for Notch2 signaling in these tumors. This hypothesis is further supported by the results of pharmacologic (GSI) and genetic (siNotch2) inhibition experiments in KNS42 cells showing that the increased activation of Notch2 in pHGG cells enhances their proliferation. An oncogenic role for Notch2 in HGGs had previously been reported only in adult tumors (Li et al. 2014; Xu et al. 2013, 2010).

These findings also reveal that the Notch2 activation documented in pHGG cells is determined epigenetically, more specifically, by the down-regulated expression of three microRNAs. Two of these (miR-107 and miR-181c) had already been shown to target the Notch2 3'UTR (Chen et al. 2013; Hashimoto et al. 2010). A luciferase reporter assay was used to validate the binding to this region of the third one: miR-29a-3p.

The effect of the down-regulation of these microRNAs was investigated only on Notch2; however, of note, other known or putative target genes of the three microRNAs, such as Bcl2, Cdc42, CDK6, CRKL, HMGA2, KLF4, PLAG1 and VEGFA are validated targets for two and putative for one of the microRNAs.

For this reason, it is not to excluded that they may affect cell proliferation in the pHGG context. Interestingly, all the three microRNAs have been reported to control proliferation in malignant gliomas in adults (Shi et al. 2017; Zhao et al. 2014) but few studies have analyzed microRNA expression in pHGGs.

Li *et al.* found that miR-107 and miR-181c were down-regulated in both high- and low-grade pediatric gliomas (Li et al. 2013).

Jha *et al.* compared microRNA expression levels in pHGGs with those found in brain tissue samples from patients operated on for epilepsy (Jha et al. 2015).

The tumor tissues were characterized by down-regulation of the miR-379/656 cluster members. Upregulated expression of several microRNAs was also observed, including those belonging to the miR-17/92 cluster, which is consistent with previous findings (Miele et al. 2014).

Eguia-Aguilar *et al.* have reported decreased expression of miR-124-3p, miR-128-1 and miR-221-3p in astrocytomas of all grades relative to levels found in normal brain tissues (Eguía-Aguilar et al. 2014). More recently, Liang *et al.* reported the down-regulation of miR-137 and miR-6500-3p in three pediatric glioma cell lines, including two that were derived from high-grade tumors (Liang et al. 2016).

In summary, these results document a link between the aberrant oncogenic pathway activation mediated by Notch2 and the down-regulated expression of miR-107, miR-181c, and miR-29a-3p suggesting that this network is a key regulator of pHGG cell growth.

Chapter 8

Conclusions

Data shown in this thesis highlight that Notch2R is expressed in an activated form in pHGGs tumors and has a role in the control of pHGG cell growth.

In fact, pharmacological inhibition or siRNA-mediated knockdown of Notch2 in KNS42 cells significantly reduces their proliferation rates.

In addition, the hyper-activation of Notch2 signaling in pHGG cells is maintained at least in part by the down-regulated expression of three Notch2-targeting microRNAs as miR-107, miR-181c, and miR-29a-3p in KNS42 cells.

These findings have potential implications for new targeted-therapies for these tumors since the inhibition of abnormal activated pathways could be an effective therapy to overcome the high levels of morbidity and mortality underlying poor long-term outcomes.

Bibliography

Ambros, Victor. 2004. "The Functions of Animal MicroRNAs." *Nature*.

Artavanis-Tsakonas, Spyros, Matthew D. Rand, and Robert J. Lake. 1999. "Notch Signaling: Cell Fate Control and Signal Integration in Development." *Science (New York, N.Y.)* 284(5415):770–76.

Baker, Suzanne J., David W. Ellison, and David H. Gutmann. 2016. *Pediatric Gliomas as Neurodevelopmental Disorders*.

Bartel, David P. 2018. "Metazoan MicroRNAs." *Cell* 173(1):20–51.

Betel, Doron, Anjali Koppal, Phaedra Agius, Chris Sander, and Christina Leslie. 2010. "Comprehens Modeling of MicroRNA Target Predicts Functional Non-Conserver and No-Conocal Sites.Pdf."

Betel, Doron, Manda Wilson, Aaron Gabow, Debora S. Marks, and Chris Sander. 2008. "The MicroRNA.Org Resource: Targets and Expression." *Nucleic Acids Research* 36(SUPPL.1).

Bolós, Victoria, Joaquín Grego-Bessa, and José Luis De La Pompa. 2007. "Notch Signaling in Development and Cancer." *Endocrine Reviews* 28(3):339–63.

Boulay, Jean Louis et al. 2007. "Loss of NOTCH2 Positively Predicts Survival in Subgroups of Human Glial Brain Tumors." *PLoS ONE* 2(6).

Braunstein, Steve, David Raleigh, Ranjit Bindra, Sabine Mueller, and Daphne Haas-Kogan. 2017. "Pediatric High-Grade Glioma: Current Molecular Landscape and Therapeutic Approaches." *Journal of Neuro-Oncology* 134(3):541–49.

Bray, Sarah J. 2006. "Notch Signalling : A Simple Pathway Becomes Complex." 7(September):678–89.

Capaccione, Kathleen M. and Sharon R. Pine. 2013. "The Notch Signaling Pathway

as a Mediator of Tumor Survival." 34(7):1420–30.

Chamdine, Omar and Amar Gajjar. 2014. "CNS Oncology Molecular Characteristics of Pediatric High-Grade Gliomas." 3:433–43.

Chen, Jie et al. 2010. "Inhibition of Notch Signaling Blocks Growth of Glioblastoma Cell Lines and Tumor Neurospheres." *Genes and Cancer* 1(8):822–35.

Chen, Lei et al. 2013. "MicroRNA-107 Inhibits Glioma Cell Migration and Invasion by Modulating Notch2 Expression." *Journal of Neuro-Oncology* 112(1):59–66.

Chen, Ricky, Adam L. Cohen, and Howard Colman. 2016. "Targeted Therapeutics in Patients With High-Grade Gliomas: Past, Present, and Future." *Current Treatment Options in Oncology* 17(8).

Chou, Chih Hung et al. 2016. "MiRTarBase 2016: Updates to the Experimentally Validated MiRNA-Target Interactions Database." *Nucleic Acids Research* 44(D1):D239–47.

Cordle, Jemima et al. 2009. "Europe PMC Funders Group Europe PMC Funders Author Manuscripts A Conserved Face of the Jagged / Serrate DSL Domain Is Involved in Notch Trans-Activation and Cis-Inhibition." 15(8):849–57.

Dawson, Mark A. and Tony Kouzarides. 2012. "Cancer Epigenetics: From Mechanism to Therapy." *Cell* 150(1):12–27.

Diaz, Alexander K. and Suzanne J. Baker. 2014. "The Genetic Signatures of Pediatric High-Grade Glioma: No Longer a One-Act Play." *Seminars in Radiation Oncology*.

Eguía-Aguilar, Pilar et al. 2014. "Reductions in the Expression of MiR-124-3p, MiR-128-1, and MiR-221-3p in Pediatric Astrocytomas Are Related to High-Grade Supratentorial, and Recurrent Tumors in Mexican Children." *Child's Nervous System* 30(7):1173–81.

El-Ayadi, Moatasem et al. 2017. "High-Grade Glioma in Very Young Children: A

Rare and Particular Patient Population." *Oncotarget* 8(38).

Fontebasso, Adam M. et al. 2014. "Recurrent Somatic Mutations in ACVR1 in Pediatric Midline High-Grade Astrocytoma." *Nature Genetics* 46(5):462–66.

Fouladi, Maryam et al. 2011. "Phase I Trial of MK-0752 in Children with Refractory CNS Malignancies: A Pediatric Brain Tumor Consortium Study." *Journal of Clinical Oncology* 29(26):3529–34.

Gajjar, Amar et al. 2015. "Pediatric Brain Tumors: Innovative Genomic Information Is Transforming the Diagnostic and Clinical Landscape." *Journal of Clinical Oncology* 33(27):2986–98.

Hashimoto, Yutaka, Yoshimitsu Akiyama, Takeshi Otsubo, Shu Shimada, and Yasuhito Yuasa. 2010. "Involvement of Epigenetically Silenced MicroRNA-181c in Gastric Carcinogenesis." *Carcinogenesis* 31(5):777–84.

J.E., Minturn and Fisher M.J. 2013. "Gliomas in Children." *Current Treatment Options in Neurology* 15(3):316–27.

Jansson, Martin D. and Anders H. Lund. 2018. "MicroRNA and Cancer." 1699.

Jha, Prerana et al. 2015. "Genome-Wide Small Noncoding RNA Profiling of Pediatric High-Grade Gliomas Reveals Deregulation of Several MiRNAs, Identifies Downregulation of SnoRNA Cluster HBII-52 and Delineates H3F3A and TP53 Mutant-Specific MiRNAs and SnoRNAs." *International Journal of Cancer* 137(10):2343–53.

Johansson, Gunnar, Ulrika Andersson, and Beatrice Melin. 2016. "Recent Developments in Brain Tumor Predisposing Syndromes." *Acta Oncologica* 55(4):401–11.

Jones, Chris et al. 2017. "Neuro-Oncology in Need of New Thinking." 19(June 2016):153–61.

Jones, Chris and Suzanne J. Baker. 2014. "Unique Genetic and Epigenetic

Mechanisms Driving Paediatric Diffuse High-Grade Glioma." *Nature Reviews Cancer* 14(10):651–61.

Juratli, Tareq A., Nan Qin, Daniel P. Cahill, and Mariella G. Filbin. 2018. "Molecular Pathogenesis and Therapeutic Implications in Pediatric High-Grade Gliomas." *Pharmacology and Therapeutics* 182:70–79.

Kallappagoudar, Satish, Rajesh K. Yadav, Brandon R. Lowe, and Janet F. Partridge. 2015. "Histone H3 Mutations—a Special Role for H3.3 in Tumorigenesis?" *Chromosoma* 124(2):177–89.

Kopan, Raphael and Ma Xenia G. Ilagan. 2010. "NIH Public Access." 137(2):216–33.

Kopan, Raphael and Ma Xenia G. Ilagan. 2009. "The Canonical Notch Signaling Pathway: Unfolding the Activation Mechanism." *Cell* 137(2):216–33.

Lasky, Joseph L. and Hong Wu. 2005. "Notch Signaling, Brain Development, and Human Disease." *Pediatric Research* 57(5):104R–109R.

Laug, Dylan, Stacey M. Glasgow, and Benjamin Deneen. 2018. "A Glial Blueprint for Gliomagenesis." *Nature Reviews Neuroscience* 19(7):393–403.

Di Leva, Gianpiero and Carlo M. Croce. 2015. "The Role of MicroRNAs in Cancer." *Targeted Therapy in Translational Cancer Research* (November 2015):80–88.

Li, Qifeng et al. 2013. "MiR-92b Inhibitor Promoted Glioma Cell Apoptosis via Targeting DKK3 and Blocking the Wnt/Beta-Catenin Signaling Pathway." *Journal of Translational Medicine* 11(1):1–9.

Li, Xuezhen, Xin He, Wei Tian, and Jianzhen Wang. 2014. "Short Hairpin RNA Targeting Notch2 Inhibits U87 Human Glioma Cell Proliferation by Inducing Cell Cycle Arrest and Apoptosis in Vitro and in Vivo." *Molecular Medicine Reports* 10(6):2843–50.

Liang, M. L. et al. 2016. "Downregulation of MiR-137 and MiR-6500-3p Promotes Cell Proliferation in Pediatric High-Grade Gliomas." *Oncotarget* 7(15):19723–37.

Llaguno, Sheila R. Alcantar. and Luis F. Parada. 2016. "Cell of Origin of Glioma: Biological and Clinical Implications." *British Journal of Cancer* 115(12):1445–50.

Louis, David N. et al. 2016. "The 2016 World Health Organization Classification of Tumors of the Central Nervous System: A Summary." *Acta Neuropathologica* 131(6):803–20.

Louvi, Angeliki and Spyros Artavanis-Tsakonas. 2006. "Notch Signalling in Vertebrate Neural Development." *Nature Reviews Neuroscience* 7(2):93–102.

Lulla, Rishi R., Amanda Muhs Saratsis, and Rintaro Hashizume. 2016. "Mutations in Chromatin Machinery and Pediatric High-Grade Glioma." *Science Advances* 2(3):1–10.

Mackay, Alan et al. 2017. "Integrated Molecular Meta-Analysis of 1,000 Pediatric High-Grade and Diffuse Intrinsic Pontine Glioma." *Cancer Cell* 32(4):520–537.e5.

Mao, Zhifu et al. 2014. "Blocking the NOTCH Pathway Can Inhibit the Growth of CD133-Positive A549 Cells and Sensitize to Chemotherapy." *Biochemical and Biophysical Research Communications*.

Maze, Ian, Kyung Min Noh, and C. David Allis. 2013. "Histone Regulation in the CNS: Basic Principles of Epigenetic Plasticity." *Neuropsychopharmacology* 38(1):3–22.

Miele, Evelina et al. 2014. "High-Throughput MicroRNA Profiling of Pediatric High-Grade Gliomas." *Neuro-Oncology* 16(2):228–40.

Munhoz de Paula Alves Coelho, Karina, Jaqueline Stall, Hercílio Fronza Júnior, Rodrigo Blasius, and Paulo Henrique Condeixa de França. 2017. "Evaluation of Expression of Genes CADM1, TWIST1 and CDH1 by Immunohistochemestry in Melanocytic Lesions." *Pathology Research and Practice* 213(9):1067–71.

Naidu, Srivatsava, Peter Magee, and Michela Garofalo. 2015. "MiRNA-Based

Therapeutic Intervention of Cancer." *Journal of Hematology and Oncology* 8(1):1–8.

Nowell, Craig S. and Freddy Radtke. 2017. "Notch as a Tumour Suppressor." *Nature Reviews Cancer* 17(3):145–59.

Ostrom, Quinn T. et al. 2015. "Alex's Lemonade Stand Foundation Infant and Childhood Primary Brain and Central Nervous System Tumors Diagnosed in the United States in 2007-2011." *Neuro-Oncology* 16(September):1–35.

Ostrom, Quinn T. et al. 2017. "CBTRUS Statistical Report: Primary Brain and Other Central Nervous System Tumors Diagnosed in the United States in 2010–2014." *Neuro-Oncology* 19(suppl_5):1–88.

Pancewicz, Joanna and Christophe Nicot. 2011. "Current Views on the Role of Notch Signaling and the Pathogenesis of Human Leukemia." *BMC Cancer* 11(1):502.

Phillips, Heidi S. et al. 2006. "Molecular Subclasses of High-Grade Glioma Predict Prognosis, Delineate a Pattern of Disease Progression, and Resemble Stages in Neurogenesis." *Cancer Cell* 9(3):157–73.

Po, A. et al. 2017. "Noncanonical GLI1 Signaling Promotes Stemness Features and in Vivo Growth in Lung Adenocarcinoma." *Oncogene* 36(32):4641–52.

Po, Agnese et al. 2017. "β-Arrestin1/MiR-326 Transcription Unit Is Epigenetically Regulated in Neural Stem Cells Where It Controls Stemness and Growth Arrest." *Stem Cells International* 2017.

Purow, Benjamin W. et al. 2005. "Expression of Notch-1 and Its Ligands, Delta-like-1 and Jagged=1, Is Critical for Glioma Cell Survival and Proliferation." *Cancer Research* 65(6):2353–63.

Schwartzentruber, Jeremy et al. 2012. "Driver Mutations in Histone H3.3 and Chromatin Remodelling Genes in Paediatric Glioblastoma." *Nature*

482(7384):226–31.

Shi, Cuijuan et al. 2017. "MiR-29a/b/c Function as Invasion Suppressors for Gliomas by Targeting CDC42 and Predict the Prognosis of Patients." *British Journal of Cancer* 117(7):1036–47.

De Smaele, Enrico, Elisabetta Ferretti, and Alberto Gulino. 2010. "MicroRNAs as Biomarkers for CNS Cancer and Other Disorders." *Brain Research* 1338:100–111.

Stockhausen, Marie Thérése, Karina Kristoffersen, and Hans Skovgaard Poulsen. 2010. "The Functional Role of Notch Signaling in Human Gliomas." *Neuro-Oncology*.

Sturm, Dominik, Stefan M. Pfister, and David T. W. W. Jones. 2017. "Pediatric Gliomas: Current Concepts on Diagnosis, Biology, and Clinical Management." *Journal of Clinical Oncology* 35(21):2370–77.

Teodorczyk, Marcin and Mirko H. H. Schmidt. 2015. "Notching on Cancer's Door: Notch Signaling in Brain Tumors." *Frontiers in Oncology* 4(January):1–14.

Weinberg, Daniel N., C. David Allis, and Chao Lu. 2017. "Oncogenic Mechanisms of Histone H3 Mutations." *Cold Spring Harbor Perspectives in Medicine*.

Wu, Gang et al. 2012. "Somatic Histone H3 Alterations in Pediatric Diffuse Intrinsic Pontine Gliomas and Non-Brainstem Glioblastomas." *Nature Genetics* 44(3):251–53.

Wu, Gang et al. 2014. "The Genomic Landscape of Diffuse Intrinsic Pontine Glioma and Pediatric Non-Brainstem High-Grade Glioma." *Nature Genetics*.

Xu, Peng et al. 2013. "The Different Role of Notch1 and Notch2 in Astrocytic Gliomas." *PLoS ONE* 8(1):1–9.

Xu, Peng et al. 2010. "The Oncogenic Roles of Notch1 in Astrocytic Gliomas in Vitro and in Vivo." *Journal of Neuro-Oncology* 97(1):41–51.

Yoon, Keejung and Nicholas Gaiano. 2005. "Notch Signaling in the Mammalian

Central Nervous System: Insights from Mouse Mutants." *Nature Neuroscience* 8(6):709–15.

Yuan, Xun et al. 2015. "Notch Signaling: An Emerging Therapeutic Target for Cancer Treatment." *Cancer Letters* 369(1):20–27.

Zhao, Dan et al. 2014. "Heat Shock Protein 47 Regulated by MiR-29a to Enhance Glioma Tumor Growth and Invasion." *Journal of Neuro-Oncology* 118(1):39–47.